Chem Soc Rev

REVIEW ARTICLE

View Article Online
View Journal | View Issue

Check for updates

Cite this: *Chem. Soc. Rev.*, 2024, **53**, 1592

Multiple hydrogen bonding driven supramolecular architectures and their biomedical applications

Yanxia Liu,†[a] Lulu Wang,†[b] Lin Zhao,[a] Yagang Zhang, *[a] Zhan-Ting Li *[cd] and Feihe Huang *[ef]

Received 15th October 2023

DOI: 10.1039/d3cs00705g

rsc.li/chem-soc-rev

Supramolecular chemistry combines the strength of molecular assembly *via* various molecular interactions. Hydrogen bonding facilitated self-assembly with the advantages of directionality, specificity, reversibility, and strength is a promising approach for constructing advanced supramolecules. There are still some challenges in hydrogen bonding based supramolecular polymers, such as complexity originating from tautomerism of the molecular building modules, the assembly process, and structure versatility of building blocks. In this review, examples are selected to give insights into multiple hydrogen bonding driven emerging supramolecular architectures. We focus on chiral supramolecular assemblies, multiple hydrogen bonding modules as stimuli responsive sources, interpenetrating polymer networks, multiple hydrogen bonding assisted organic frameworks, supramolecular adhesives, energy dissipators, and quantitative analysis of nano-adhesion. The applications in biomedical materials are focused with detailed examples including drug design evolution for myotonic dystrophy, molecular assembly for advanced drug delivery, an indicator displacement strategy for DNA detection, tissue engineering, and self-assembly complexes as gene delivery vectors for gene transfection. In addition, insights into the current challenges and future perspectives of this field to propel the development of multiple hydrogen bonding facilitated supramolecular materials are proposed.

Published on 03 January 2024. Downloaded by Yunnan University on 8/4/2025 1:35:41 AM.

1. Introduction

Supramolecular polymers are the exciting spinoffs of polymer and supramolecular science. They are known for their dynamic, reversible, stimulus responsive, and versatile features. Supramolecular polymers formed and assembled with non-covalent bonds become a hot topic of chemical science because of their special structures and properties.[1,2] In supramolecular systems, the bond energy of host–guest interactions based on weak interactions between molecules or secondary bonds is about 5–10% of the covalent bond energy.[3] It mainly studies molecular interactions between monomers through different non-covalent interactions, for instance π–π stacking, hydrogen bonding, ion-dipole, metal–ligand *etc.* (Fig. 1A).[4,5] Molecular aggregates are formed through the coordination of these intermolecular forces and space complementarity. These weak interactions govern the assembly of extensive aspects from the double helix in DNA to the bonding of H_2O molecules in liquid water.[6] The synergy, directionality, and selectivity of various forces determine the validity of the molecular recognition process. Supramolecular polymers possess high recognition ability and can achieve many complex and advanced functions.[7,8]

The interaction energy of a hydrogen bond ranges from 5 to 120 kJ mol^{-1} (Fig. 1A).[5,9] A hydrogen bond denoted as X–H···Y is an electrostatic interaction between a hydrogen bonding donor ("D", a hydrogen atom in a polar bond) and a hydrogen bonding acceptor ("A", a strongly electronegative atom with a lone pair available for bonding, typically O, N, or F). Individual hydrogen bonds are weak, while multiple hydrogen bonds, as well as synergies with other non-covalent interactions, can form high strength supramolecular aggregates. Increasing multiple hydrogen bonding motifs can improve the strength and diversity of the stimulus response of supramolecular polymers.[10]

[a] *School of Materials and Energy, University of Electronic Science and Technology of China, Chengdu 611731, Sichuan, China. E-mail: ygzhang@uestc.edu.cn*
[b] *State Key Laboratory of Chemistry and Utilization of Carbon-based Energy Resource, Xinjiang University, Urumqi, Xinjiang 830046, China*
[c] *Key Laboratory of Synthetic and Self-Assembly Chemistry for Organic Functional Molecules, Shanghai Institute of Organic Chemistry (SIOC), Chinese Academy of Sciences, Shanghai 200032, China*
[d] *Department of Chemistry, Shanghai Key Laboratory of Molecular Catalysis and Innovative Materials, Fudan University, 2205 Songhu Road, Shanghai 200438, China. E-mail: ztli@fudan.edu.cn*
[e] *Stoddart Institute of Molecular Science, Department of Chemistry, Zhejiang University, Hangzhou 310058, China. E-mail: fhuang@zju.edu.cn*
[f] *ZJU-Hangzhou Global Scientific and Technological Innovation Center–Hangzhou Zhijiang Silicone Chemicals Co. Ltd. Joint Lab, Zhejiang-Israel Joint Laboratory of Self-Assembling Functional Materials, ZJU-Hangzhou Global Scientific and Technological Innovation Center, Zhejiang University, Hangzhou 311215, China*
† These authors contributed equally.

This journal is © The Royal Society of Chemistry 2024

Published on 03 January 2024. Downloaded by Yunnan University on 8/4/2025 1:35:41 AM.

When hydrogen bonds are arranged in order to form double, triple, quadruple or even larger hydrogen bonding systems, the synergistic and superimposed effects of multiple hydrogen bonding significantly improve the binding energy for bond cooperation and construct highly selective and specific pairing forms.[11] Some groups not only form complementary multiple hydrogen bonds by themselves, but also form complementary multiple hydrogen bonds with other groups, which enriches the types of multiple hydrogen bonds. Substantial secondary electrostatic interactions, attractive or repulsive ones between adjacent sites in hydrogen bonding complexes, significantly contribute to complex stability and promote or even offset the effect of extra hydrogen bonds (Fig. 1B).[12–15]

In nature, adhesion is usually driven by reversible interactions at the molecular level.[16] These interactions are controlled by stimuli, either from the environment or from the organism, to meet specific needs. Nature controls adhesion and acquires complex functions through a variety of non-covalent interactions.[17–20] Hydrogen bond motifs are most widely used for achieving reversible bonding and debonding,[21] possibly because hydrogen bonding units are easily introduced into polymeric structures or reactive monomers.[22–24]

In both biological systems and industrial applications, adhesive interactions have important effects on their surface binding. Designing intermolecular and intramolecular hydrogen bond networks to construct high strength polymer materials is an important bio-inspired strategy.[25] Small molecules or polymers with multiple hydrogen bonds are effective building blocks to construct multifunctional supramolecular adhesives and advanced molecular architecture.[26,27] For nano-adhesion, multiple hydrogen bonds can enhance the overall adhesive forces between surfaces. The presence of multiple hydrogen bonds in nano-adhesives provides opportunities to improve the adhesion performance, resistance to mechanical stress, and longevity of nano-adhesive materials. Supramolecular systems based on hydrogen bonding are promising with great potential

Yanxia Liu

Yanxia Liu is a postdoctoral researcher at the School of Materials and Energy, University of Electronic Science and Technology of China. She obtained her PhD from the Xinjiang Technical Institute of Physics and Chemistry, Chinese Academy of Sciences, in 2021. Currently she is a Postdoc at UESTC under the guidance of Prof. Yagang Zhang. Her research interests include the design and synthesis of advanced functional materials and polymer composites for various applications.

Lulu Wang

Lulu Wang is an associate professor at the School of Chemistry, Xinjiang University. She obtained her PhD degree from the Xinjiang Technical Institute of Physics and Chemistry, Chinese Academy of Sciences, under the direction of Prof. Yagang Zhang in 2019. Her research interest is focused on functional monomer design, supramolecular polymer design, and molecular recognition and imprinting.

Lin Zhao

Lin Zhao is a lecturer at the University of Electronic Science and Technology of China. She obtained her MS degree from the University of Electronic Science and Technology of China in 2009. Her research interest is focused on green chemistry and clean processes based on molecular recognition and molecular imprinting.

Yagang Zhang

Yagang Zhang is a professor at the University of Electronic Science and Technology of China. He obtained his PhD from the University of South Carolina in 2010. He worked as a Postdoc Research Associate at the University of Illinois at Urbana-Champaign from 2010 to 2013. He served as the Director of Xinjiang Fine Chemical Engineering Research Center from 2014 to 2019. He joined UESTC in 2019 as a full professor and group leader of the chemistry materials lab. He is Fellow of the Royal Society of Chemistry and a Grand Board Member of the Chinese Chemical Society. His research focuses on functional oriented molecular recognition and assembly for the design and development of advanced functional materials.

Published on 03 January 2024. Downloaded by Yunnan University on 8/4/2025 1:35:41 AM.

application prospects, ranging from nanoelectronics and biomaterials to coatings and adhesive technologies, due to their directionality, reversibility, and specificity.[28–32]

Most reviews on supramolecular polymers are about their synthesis, properties, and applications. Instead of providing a comprehensive review, here we focus on bio-inspired hydrogen bonding driven supramolecular architectures and their biomedical applications.[2,10,13,33–46]

This review focuses on the design and development of emerging supramolecular architectures based on multiple hydrogen bonding interactions, especially highlighting studies on biomedical applications mainly published in recent years. Firstly, we provide an overview of hydrogen bonding systems, which prompts us to understand the development and principles of motifs' design. Then the pathway complexity of multiple hydrogen bonding pairs and structure versatility of building blocks are discussed. Furthermore, several emerging hydrogen bonding supramolecular architectures are highlighted. In addition, multiple hydrogen bonding modules as energy dissipators and quantitative analysis of nano-adhesion are also described. These help us to understand the structure–property relationships more deeply. Finally, we highlight the application of multiple hydrogen bonding stimulated supramolecular architectures in biomedical materials.

2. Multiple hydrogen bonding systems and nano-adhesion

2.1 The power of the genetic code

Hydrogen bonding interactions are key to the genetic code and are ubiquitous in natural systems. DNA forms a double helix through hydrogen bonds, paired by double and triple hydrogen bonds, respectively, between the purine and pyrimidine nucleic acid bases. RNA-specific uracil replaces thymine in DNA and pairs with adenine when DNA is transcribed (Fig. 2).[47] The hydrogen bonds in these two groups are parallel and the bond lengths are similar (0.29 nm) and adjacent atoms form approximate planar hexagons. The triple hydrogen bonding complex guanine–cytosine (G–C) has a notable association constant (K_a) of 10^4–10^5 M^{-1} in $CHCl_3$,[48] much higher than a K_a of 130 M^{-1} and 100 M^{-1} observed for complexes adenine–thymine (A–T) and adenine–uracil (A–U), as well as others between adenine and uracil derivatives (K_a < 220 M^{-1}) with two hydrogen bonds.[49] Thus, nature selected hydrogen bonding motifs within base pairs, enabling the transmission of genetic information to be transcribed in a simple and precise manner.

In addition, hydrogen bonding interactions have great influence on the properties and performance of materials. Spider dragline silk exhibits excellent mechanical properties due to its multiple hydrogen bonds and is the toughest natural fiber known. A single hydrogen bond is weak and usually cannot form stable self-assembled structures. Inspired by the elegant design of nature, multiple hydrogen bonds can increase the interaction energy and achieve nano-adhesion through reasonable design, enabling the elegant modulation of materials properties.[5]

2.2 Double and triple hydrogen bonding systems

Hydrogen bonding donors and receptors can form two types of double hydrogen bond arrays, AA–DD and AD–DA. Sherrington *et al.*[50] reported that 2-acrylamidopyridine can self-associate by hydrogen bonding, and the association constant is temperature-dependent (Fig. 3).[33]

Compared with the double hydrogen bonding systems, the triple hydrogen bonding systems (AAA–DDD, AAD–DDA, and ADA–DAD, Fig. 1B) can form stronger networks. Zimmerman's group[51] designed a series of triple hydrogen bonding complexes (Fig. 4): ADA–DAD dimers 1·2 (K_a = 78 M^{-1} in $CHCl_3$, Fig. 4A) and 1·3 (K_a = 70 M^{-1} in $CHCl_3$ Fig. 4B) with four

Zhan-Ting Li

Zhan-Ting Li received his BS from Zhengzhou University in 1985 and his PhD with Qing-Yun Chen at the Shanghai Institute of Organic Chemistry in 1992. He carried out postdoctoral research with Jan Becher at the University of South Denmark and Steven C. Zimmerman at the University of Illinois at Urbana-Champaign. He worked as a PI at SIOC (1995–2010) and is currently is a Professor at the Department of Chemistry, Fudan University and PI at SIOC. His research interests include porous organic and supramolecular materials, macrocycles and molecular cages for biological applications and photocatalysis.

Feihe Huang

Feihe Huang is a Changjiang Scholar Chair Professor of Zhejiang University. His current research is focused on supramolecular polymers and nonporous adaptive crystals (NACs). Awards and honours he has received include Chinese Chemical Society AkzoNobel Chemical Sciences Award, The Cram Lehn Pedersen Prize in Supramolecular Chemistry, Royal Society of Chemistry Polymer Chemistry Lectureship award, and Bruno Werdelmann Lectureship Award. His publications have been cited more than 32 476 times. His h-index is 98. He sits/sat on the Advisory Boards of JACS, Chem Soc Rev, ChemCommun, Macromolecules, ACS Macro Lett., and Polym. Chem. He is an Editorial Board Member of Mater. Chem. Front.

 This journal is © The Royal Society of Chemistry 2024

Published on 03 January 2024. Downloaded by Yunnan University on 8/4/2025 1:35:41 AM.

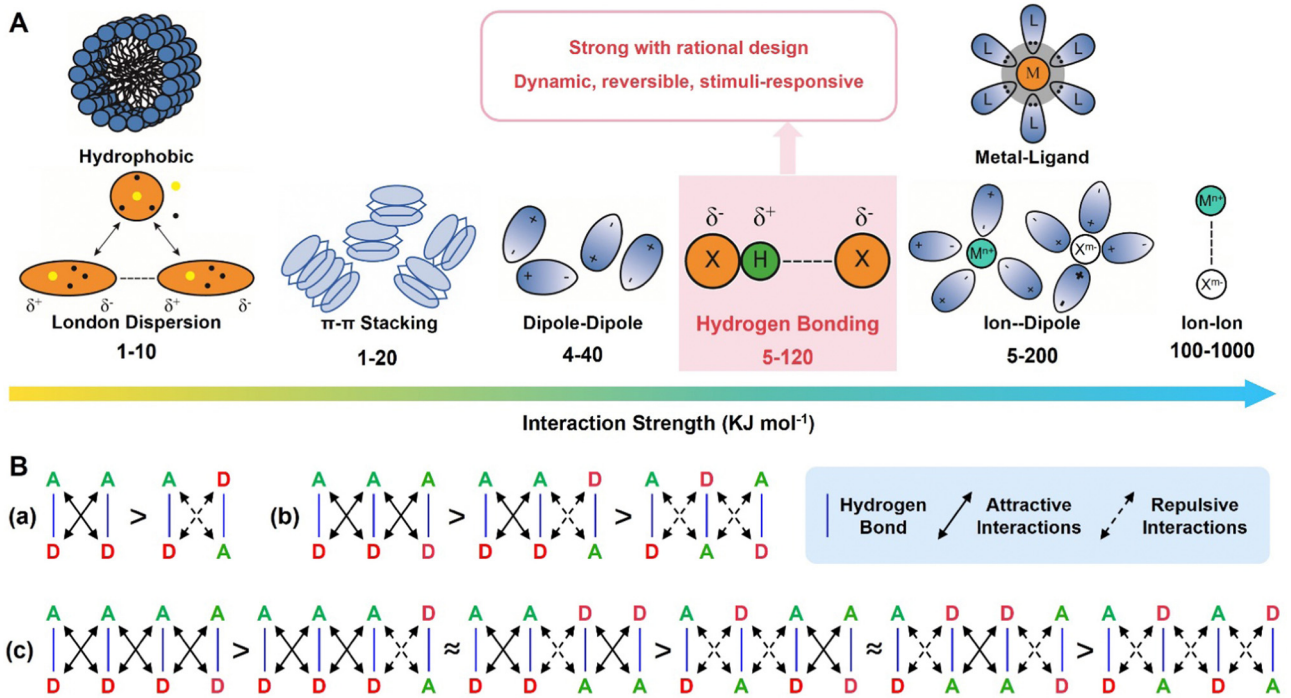

Fig. 1 (A) The interaction energy of some non-covalent interactions.[5] (B) The primary attractive hydrogen bonds and secondary electrostatic interactions between proton donors (**D**, red) and acceptors (**A**, green) in (a) double, (b) triple, and (c) quadruple hydrogen bonding arrays.[12–15]

repulsive secondary interactions,[52,53] AAD–DDA dimers 4·5 (K_a = 10^4 M^{-1} in $CHCl_3$, Fig. 4C) and 6·7 (K_a = 9.3 × 10^3 M^{-1} in $CHCl_3$, Fig. 4D) with medium secondary interactions and AAA–DDD dimer 8·9 (K_a > 10^5 M^{-1} in $CHCl_3$, Fig. 4E) with four attractive secondary interactions. The K_a of the AAA–DDD dimer was much higher than that of the ADA–DAD dimer. DDD unit 9 is unstable under acidic conditions and becomes readily prototropic to exist in the noncomplementary form.[54] DDD unit 10 has a cationic charge character and the K_a of complex 8·10 (Fig. 4F) exceeds 5 × 10^5 M^{-1} in CH_2Cl_2.[55] The K_a of complex 11·12 (Fig. 4G) is 2 × 10^7 M^{-1} in CH_2Cl_2 and that of complex 11·13 (Fig. 4H) is 3 × 10^{10} M^{-1} with the highest stability.[56,57] The K_a of complex 12·14 (Fig. 4I) is 1.1 × 10^7 M^{-1} in CH_2Cl_2.[58]

2.3 Quadruple hydrogen bonding systems

The binding strength of quadruple hydrogen bonding units, and their predictable and controllable recognition performance, has attracted widespread attention for their applicability to the construction of stimuli responsive assemblies, nanofibers, supramolecular polymers, *etc.*[59–65] There are six different quadruple hydrogen bonding dimers, DDDD–AAAA, DDDA–AAAD, DDAD–AADA, DDAA–AADD, DADA–ADAD and DAAD–ADDA (Fig. 1B).[12] Self-complementary DDAA and DADA arrays have advantages in the self-assembly of supramolecular polymers, although they may limit their recognition ability.[14]

Meijer's group[15] focused on the synthesis of an ureidopyrimidinone (UPy) functionality containing quadruple hydrogen bonds. UPy–UPy is easy to synthesis and possesses a high K_a of 6 × 10^7 M^{-1} in $CDCl_3$ (Fig. 5A). Functionalization of the termini of telechelic polymers with quadruple hydrogen bonding UPy units enables access to the selective formation of long linear chains, thus improving the properties of the material.[66,67] The tautomerism in the self-assembly process of UPy leads to cross recognition and affects the specificity of recognition.[68–73] For the linear identification unit, the order of hydrogen bonds in the donor and acceptor should be guaranteed to minimize the tendency of self-aggregation. Zimmerman's group[54,73–76] developed quadruple hydrogen bonding units, such as deazapterin (DeAP) (Fig. 5B), 2,7-diamido-1,8-naphthyridine (DAN) (Fig. 5C),[75] butyl urea of guanosine (UG) (Fig. 5D), and 7-deazaguanine-based

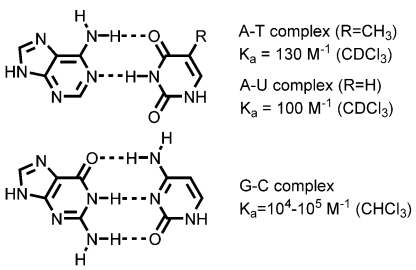

Fig. 2 Watson–Crick coupling pairs and association constants in DNA (A–T and G–C) and RNA (A–U) molecules.[45]

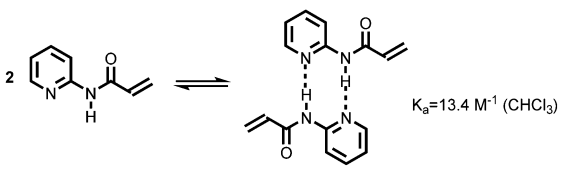

Fig. 3 Self-association of 2-acrylaminopyridine.[31]

Published on 03 January 2024. Downloaded by Yunnan University on 8/4/2025 1:35:41 AM.

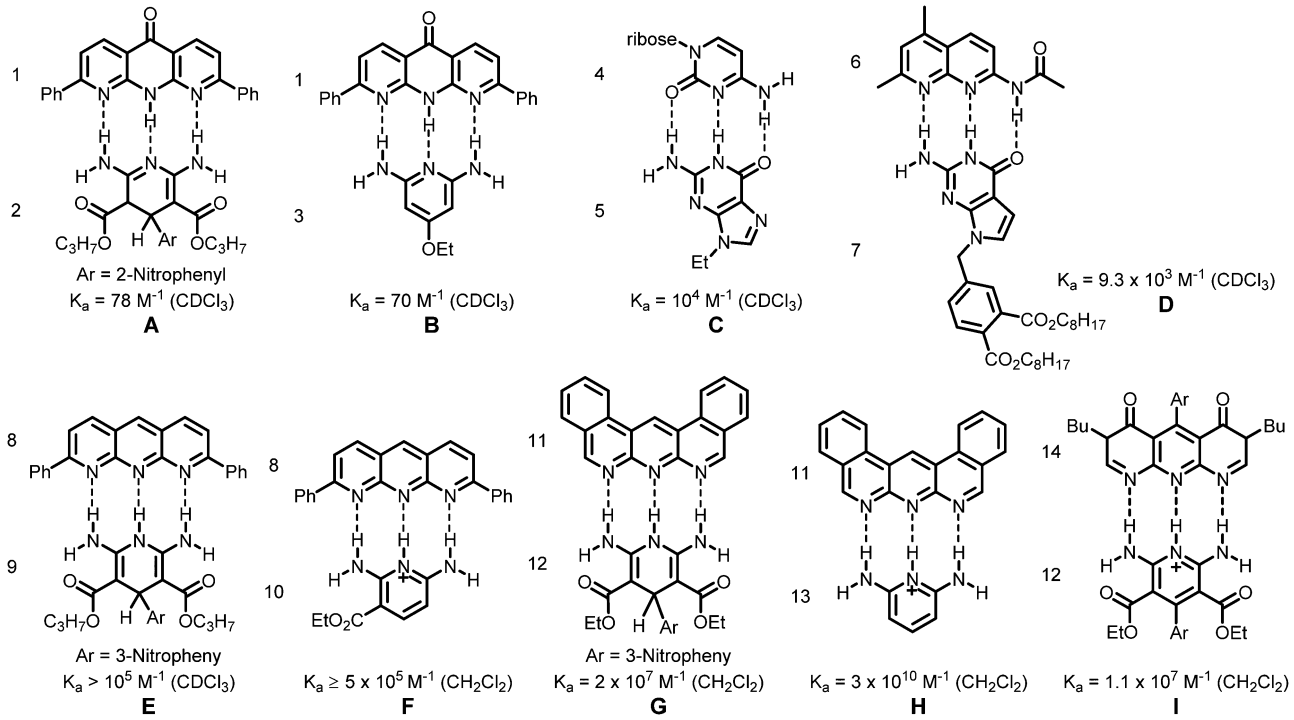

Fig. 4 Structures and association constants of triple hydrogen bonding complexes.[51–58]

urea (DeUG) (Fig. 5D). The self-association constants of DAN (10–70 M^{-1}) and UG (200–300 M^{-1}) are much weaker, while the K_a of DAN–UG is as high as 5×10^7 M^{-1} in $CDCl_3$ (Fig. 5D).[72,75,77] The self-association constant of DeUG is 880 M^{-1} and the K_a of DAN–DeUG reaches up to 2×10^8 M^{-1} in $CDCl_3$ (Fig. 5D).[76] Fig. 5E and F shows the structure of some other quadruple hydrogen bonding complexes, and their K_a values are much lower than the expected values. This is because K_a is affected by undesired folded conformers and tautomeric equilibrium, the connected substituents and the linker between neighbouring hydrogen bonds.[78–80]

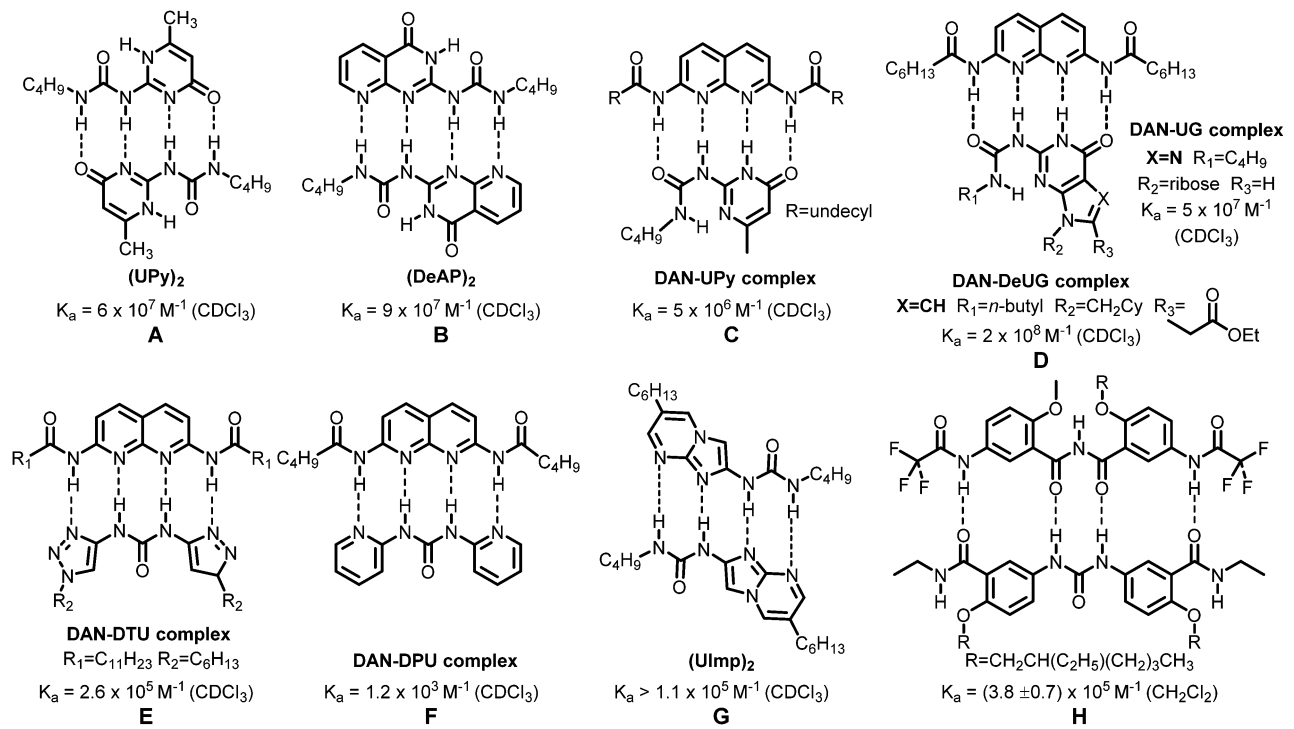

Fig. 5 Structures and association constants of quadruple hydrogen bonding complexes.[66,73–80]

 This journal is © The Royal Society of Chemistry 2024

Published on 03 January 2024. Downloaded by Yunnan University on 8/4/2025 1:35:41 AM.

2.4 Multiple hydrogen bonding systems

Multiple hydrogen bonding systems are difficult to synthesize because of their higher binding constants. If there are too many hydrogen bonds, it becomes difficult for all hydrogen bonds to be coplanar. In particular, the position and orientation of hydrogen bonds are pre-designed using the intramolecular hydrogen bonds and the rigidity of the molecules themselves.

Hamilton *et al.*[81] synthesized a macrocyclic receptor containing six hydrogen bonds within a cavity by binding two 2,6-diamidopyridine units. The strong binding ($K_a = 2.08 \times 10^4$ M^{-1} in $CDCl_3$, Fig. 6A) and recognition of barbiturate derivatives was realized by the ADADAD–DADADA array. The K_a of the macrocyclic derivative (Fig. 6B) is 1.37×10^6 M^{-1} in $CDCl_3$ increased by 100 times, suggesting that enforced inwardly pointing binding site is considerable. Gong *et al.*[82] reported an extremely stable hextuple hydrogen bonding system (K_a = $(1.3 \pm 0.7) \times 10^9$ M^{-1} in $CHCl_3$, Fig. 6C) between two oligoamide molecular strands. The six hydrogen bond monomers remained coplanar by means of intramolecular hydrogen bonds. In nonpolar solvents, oligoamide strands can be combined in a specific order to form hydrogen bonding double duplexes, while in aqueous media, they can be converted to disulfide crosslinked duplexes.[83] In aqueous solution and methanol, oligoamide strands combined with the trityl-protected thiol group to form duplexes composed of complementary hydrogen bonding sequences. Wilson *et al.*[84] synthesized a six hydrogen bonding heterodimer (Fig. 6D) comprising ditopic ureidoimidazole and amidoisocytosine motifs, showing high stability in $CDCl_3$ ($K_a > 10^5$ M^{-1}).

Schmuck *et al.*[85] reported an efficient self-complementary system (K_a = 170 M^{-1} in water, Fig. 6E) with a water-soluble zwitterion. The zwitterion combined with two interacting ion pairs to form an extremely stable dimer linked together by a hextuple hydrogen bonding network. A neutral dimer (Fig. 6F) with solely hydrogen bonds was stable only in low polar organic solvents, with K_a above 10^4 M^{-1} in $CDCl_3$ and K_a below 10 M^{-1} in 5% DMSO-d_6/$CDCl_3$. Therefore, ion pair interactions play an important role in the stable self-association of hydrogen bonding motifs in water.

Zimmerman *et al.*[86] developed an eight contiguous hydrogen bonding ureido-naphthyridine oligomer ($K_a > 4.5 \times 10^5$ M^{-1} in 10% DMSO-d_6/$CDCl_3$, Fig. 6G), which shows a self-complementary

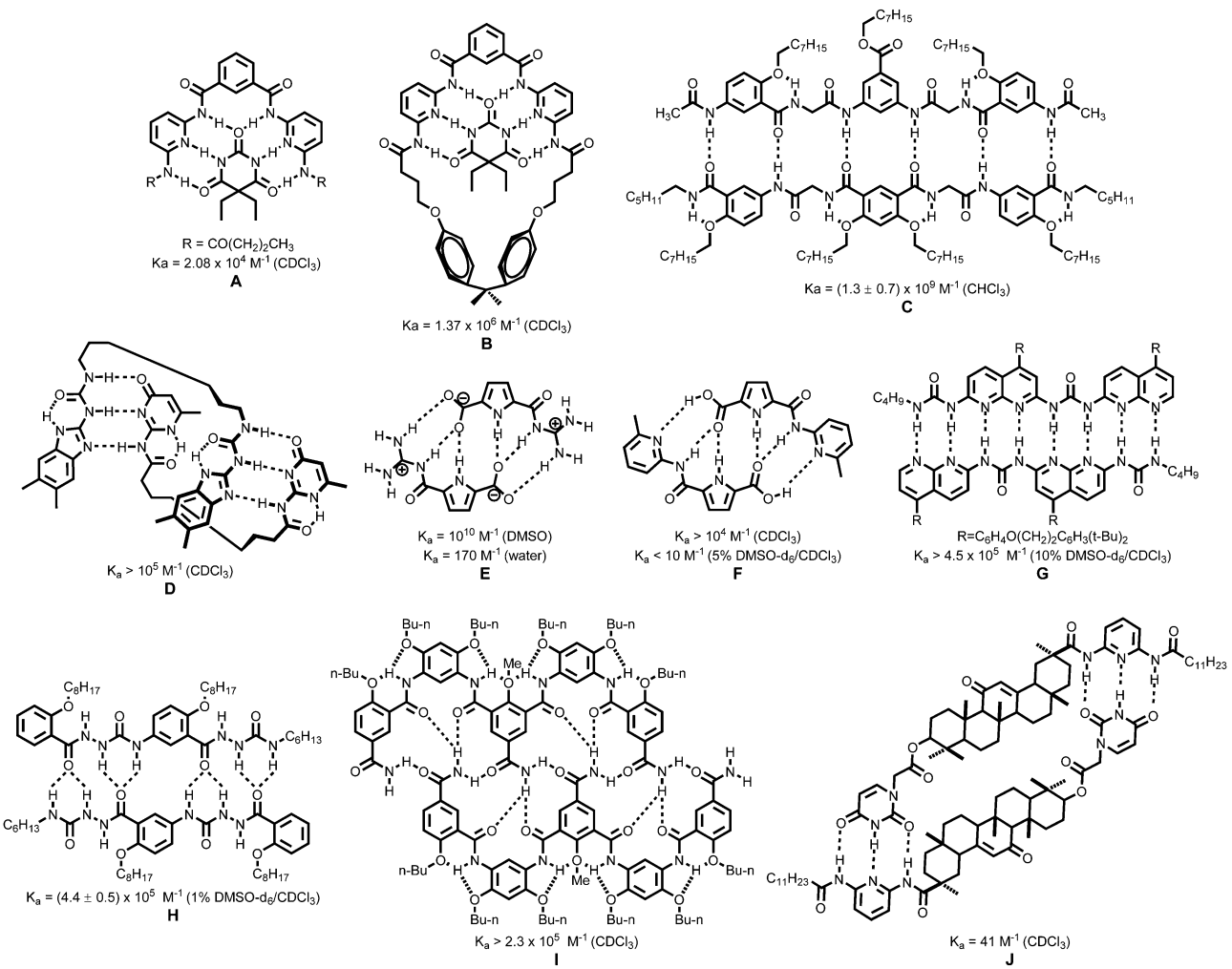

Fig. 6 Structures and association constants of multiple hydrogen bonding complexes.[81,82,84–89]

Published on 03 January 2024. Downloaded by Yunnan University on 8/4/2025 1:35:41 AM.

hydrogen bonding array (DDAADDAA). Chen *et al.*[87] reported a highly stable homoduplex within four intermolecular tricenter hydrogen bonds (K_a = (4.4 ± 0.5) × 10^4 M^{-1} in 1% DMSO-d_6/$CDCl_3$,Fig. 6H) in low polar solvents. Li *et al.*[88] presented a monomer (Fig. 6I) possessing a rigidified anthranilamide skeleton. Intermolecular hydrogen bonds are formed by introducing amide units into the preorganized skeleton. The non-continuous thirteen hydrogen bonding supramolecular duplex is highly stable in $CDCl_3$ (K_a > 2.3 × 10^5 M^{-1}). Ju *et al.*[89] synthesized a glycyrrhetinic acid conjugate (K_a = 41 M^{-1} $CDCl_3$, Fig. 6J) containing uracil units and 2,6-diaminopyridine. The six intermolecular hydrogen bonds formed a supramolecular cyclic dimeric structure by self-assembly. The formed cavity could recognize and encapsulate the polar molecule in aprotic polar solvents.

2.5 Molecular recognition and nano-adhesion

The adhesion phenomenon exists widely in nature. Adhesion occurs by covalent bonding or non-covalent interactions, for example, the adhesion shown by secretions of mussels (metal ligand and hydrogen bonding complexes) and gecko foot pads (van der Waals forces).[19] The adhesion phenomenon is important in adhesive materials, hydrogels, coatings, adhesives, *etc.* The surface protection ability and mechanical properties of conventional covalent adhesion systems will be decreased due to poor interfacial properties. Covalent and non-covalent interactions can improve the interfacial properties of materials synergically. According to this principle, many multi-functional coupling agents and adhesion promoters have been designed to act as bridges between the adhesive and the attachment.[90]

Inspired by bio-adhesion, nano-adhesion based on supramolecular interactions has been developed in recent years.[91] Hydrogen bonding is a common interaction in complex organisms and is exploited as a molecular interaction tool to manufacture a variety of biomimetic materials. Hydrogen bonding not only increases the adhesion and mechanical properties of polymers, but also dissipates material energy in nonpolar solvents, due to their dynamic association/dissociation. The reversible assembly of the non-covalent nano-adhesive offers the potential to guide the complexation process, resulting in reversible and self-healing adhesive materials,[92] and for decreasing permanent damage to the assembled elements and for increased sustainability.[93]

In view of industrial demand, high performance adhesives have aroused great interest. Polymeric materials possess long intertwined chains, and the introduction of multiple hydrogen bonding modules with nano-adhesion and high affinity into the polymer structure at main chains (Fig. 7A–C), end chains (Fig. 7D–F) and side chains (Fig. 7G and H)[5] can form a variety of supramolecular polymers with adhesive properties, strength and toughness. Many supramolecular nano-adhesives perform better than commercial glues and reported adhesives.[91] We believe that these synthetic polymers can become "smart" materials sensitive to stimuli such as heat, light, and mechanical forces.[94] The nano-adhesive supramolecular polymers with self-healing and scalability are expected to be applied in wearable devices, wound dressing, electronic skin, and other biomedical fields.

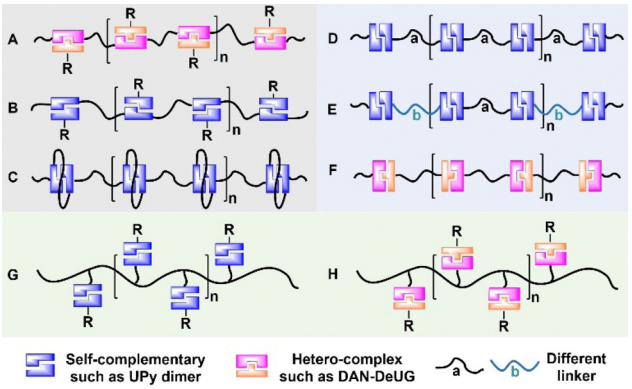

Fig. 7 Schematic representation of introducing multiple hydrogen bonding modules into the main chains (A–C), end chains (D–F) and side chains (G and H) of supramolecular polymer structures.[5]

2.6 Pathway complexity of multiple hydrogen bonding pairs

Multiple hydrogen bonding is a powerful means to synthesize advanced supramolecular architectures.[95,96] When studying the double helix structure of DNA, the alternation of hydrogen bonding structures puzzles life science workers. Heterocycles can form robust hydrogen bonding complexes in solution, but the prototropy leads to complication. It not only reduces the association constant, but also compromises the information content. The use of heterocycles is complex and is identical to intramolecular hydrogen bonding mediated molecular folding.[97,98] In the process of self-assembly, the functional monomers have tautomerism, so there is complexity in the initial design stage and the final material evaluation stage.

UPy has three tautomeric forms, 6[1*H*]-pyrimidinone tautomer (U_a), 4[1*H*]-pyrimidinone tautomer (U_b) and pyrimidinol tautomer (U_c) (Fig. 8A). The tautomerism of the UPy unit leads to self-assembly cross recognition, which makes the specificity of recognition unsatisfactory.[15,66] U_b and U_c can be dimerized *via* AADD and DADA arrays, respectively. AADD–DDAA arrays are more stable than ADAD–DADA arrays.[52] The NH group of pyrimidine and O or N atoms of urea formed a linear array of quadruple hydrogen bonds through intramolecular hydrogen bonding, which considerably enhances the stability of dimers. U_a without self-association can induce an association constant loss, which leads to defects and limits its application. Prototropy does not affect the self-association process of heterocycles. Deazapterin heterocycle DeAP (D_a) with a self-complementary hydrogen bonding array AADD has three tautomerism forms (Fig. 8B), independent of its protomeric form.[54,74] There are four homodimers and heterodimers, D_a–D_a, D_a–D_b, D_b–D_b, and D_c–D_c. These dimers are 13%, 46%, 39%, and 2% in toluene-d_8, respectively, while those in $CDCl_3$ are 40%, 43%, 11%, and 6%, respectively. UPy and DeAP formed robust hydrogen bonding complexes with DAN through ADDA forms, generating non-complementary conformers U_d, D_d, and D_e. When excess DAN was added to the solution (toluene-d_8 or $CDCl_3$) of D_a and D_b dimers, complexes with DAN can be obtained, and the dimers were completely dissociated.

This journal is © The Royal Society of Chemistry 2024

Published on 03 January 2024. Downloaded by Yunnan University on 8/4/2025 1:35:41 AM.

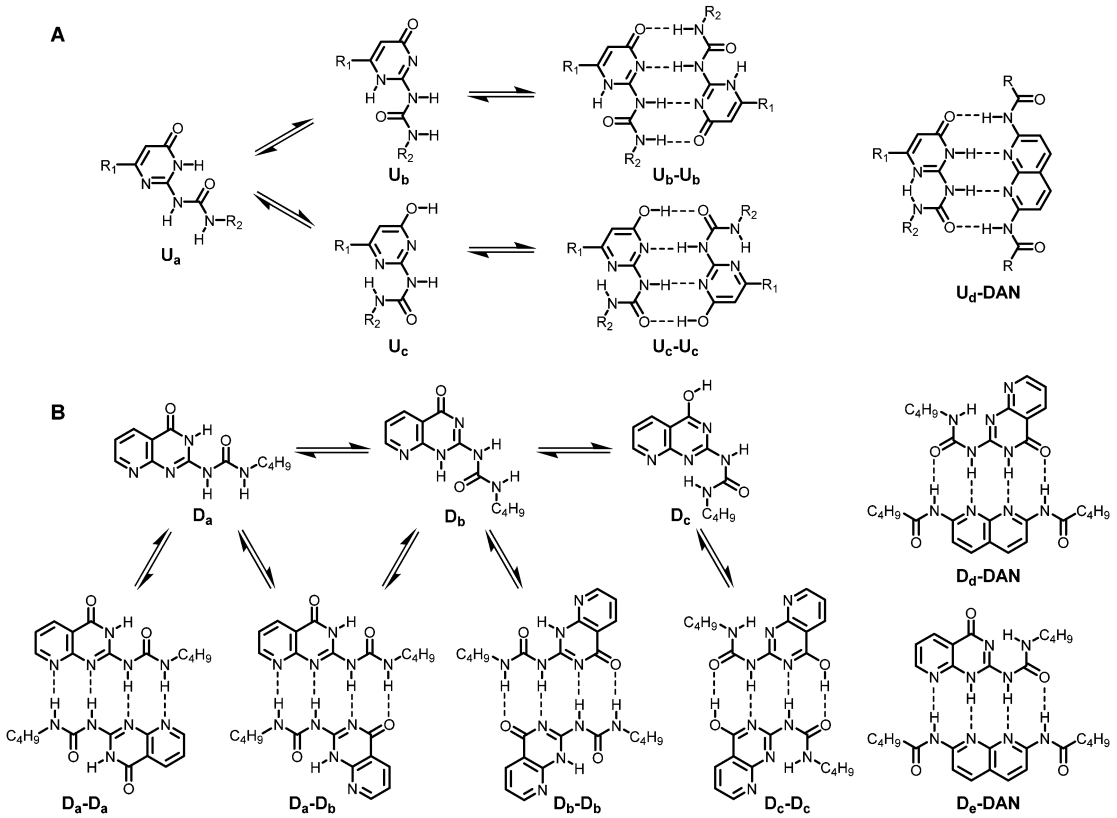

Fig. 8 Equilibria between tautomeric forms and their dimers of (A) UPy,[15] (B) DeAP,[54] and conformers induced by DAN.

Guo *et al.*[99] constructed single-molecule junctions with hydrogen bond bridges (HBB-SMJs). The quadruple hydrogen bonding system was sandwiched between graphene point contacts to form SMJs. To determine the metastable structures, possible configurations for intermolecular proton transfer reactions or tautomerism were investigated theoretically (Fig. 9). Five low-lying energy structures (Fig. 9A–E) were identified. Studies have shown the lactam–lactim tautomerism process occurs almost simultaneously, which is highly correlated with the configuration of HBB-SMJs and diphenyl ether molecules.

The pathway complexity not only exists at the molecular level in the initial assembly stage, but also later in the process to form highly ordered supramolecular aggregates and polymers. The pathway complexity in supramolecular polymerization can be mediated by the equilibrium with free monomers and temperature.[100] Meijer *et al.*[101] described a supramolecular polymer that undergoes four different conformers, two helicities (*P* and *M*) with two dihedral angle θ (45° and 35°) between the hydrogen bonding amides and the central benzene ring (Fig. 10A). 1,3,5-Benzenetricarboxamide (BTA) is a commonly used supramolecular polymer scaffold that can be directly self-assembled by hydrogen bonding and stacking of cores. (*S*,*S*,*S*)-D-BTA was self-assembled through three intermolecular amide hydrogen bonding, the stacking between benzene rings through solvophobic effects further stabilized the hydrogen bonding. Notably, hydrogen bonding affects the persistence of monomer stacking and the orderliness of supramolecular polymers.[102] Chiral centers at the side-chains of amides make aggregates exhibit helical chirality. In supramolecular polymerizations, temperature, solvent and supramolecular aggregates are very important factors.

Understanding the effect of solvents on the aggregate behavior of supramolecular modules helps us to find out how the final structures are formed.[103,104] Hierarchical self-assembly of amphiphilic BiPy–BTA discotics initially formed a supramolecular fiber and then organized into a triple helical bundle by solvent effects (Fig. 10B). With the decrease of solvent polarity, the hydrophobic force was gradually weakened, which led to the formation of a 1D fiber. Water induced the bundling of supramolecular fibers that transformed into a triple helical bundle at high water content.[105] The rich phase behaviour of the supramolecular assembly is closely related to the thermodynamics of the water–alcohol mixtures.

Self-recognition and competing equilibria may cause deleterious effects for many applications. Sanjayan *et al.*[106] utilized intramolecular bifurcated hydrogen bonding interactions and addressed the prototropy challenges of heterocyclic AADD self-assembly complexes by freezing hydrogen bonding codes. The resulting hydroquinone conjugated AADD system was characterized by a built-in fluorophore, high duplex stability and prototropy free dimerization to produce single duplexes. Clayden *et al.*[107] prepared symmetric oligourea foldamers from cyclohexane-1,2-diamine, using terminal groups (carbamate, urea, or thiourea) with different hydrogen bonding capabilities

Published on 03 January 2024. Downloaded by Yunnan University on 8/4/2025 1:35:41 AM.

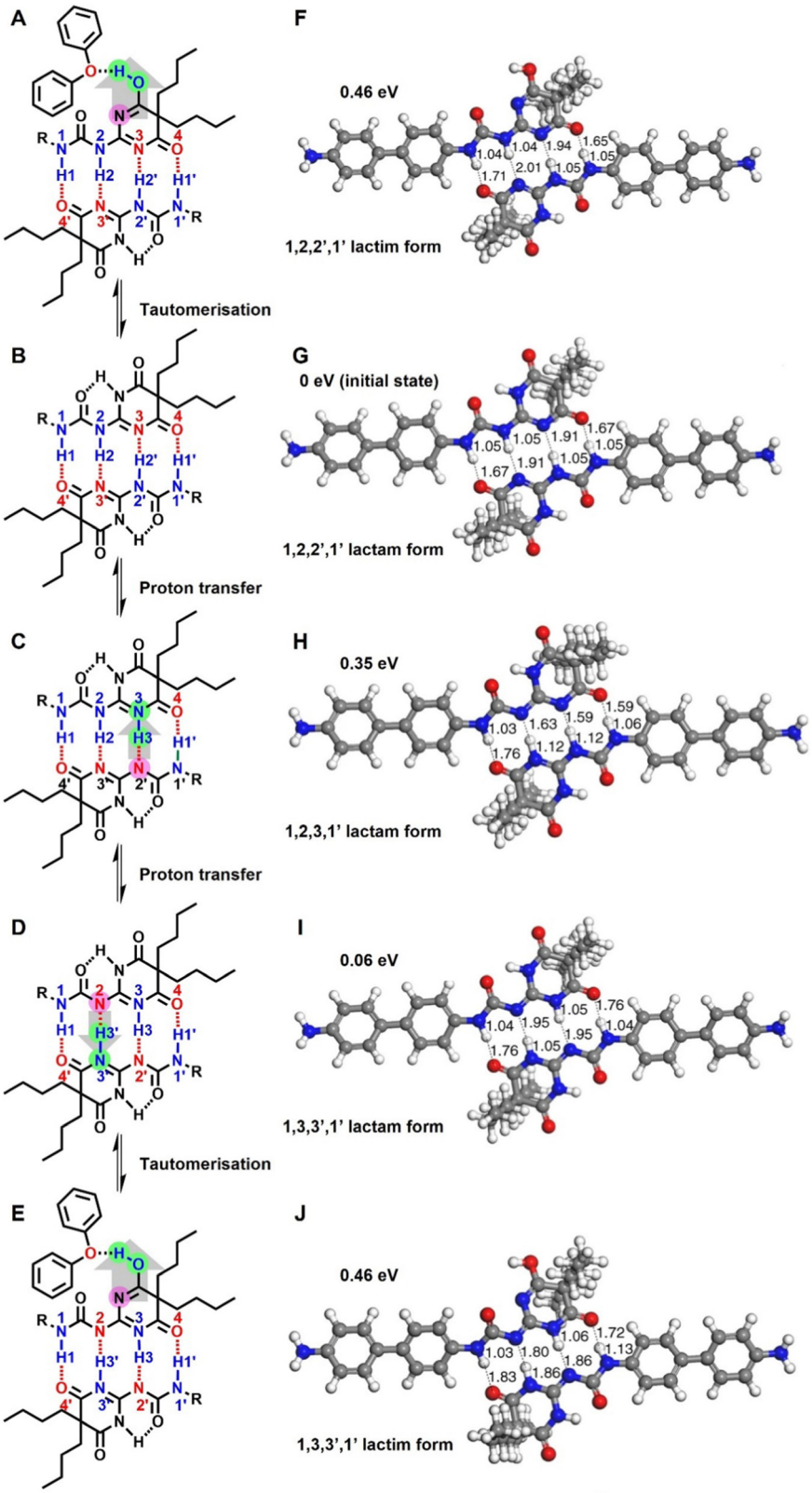

Fig. 9 Schematic representation of hydrogen bond transformations (A)–(E) and low-lying energy structures (F)–(J).[99]

to desymmetrize. The foldamers were dynamically balanced between the two-alternative screw-sense configurations (Fig. 10C) and are solvent independent. The hydrogen bonding properties of the terminal groups determined the relative

 This journal is © The Royal Society of Chemistry 2024

Published on 03 January 2024. Downloaded by Yunnan University on 8/4/2025 1:35:41 AM.

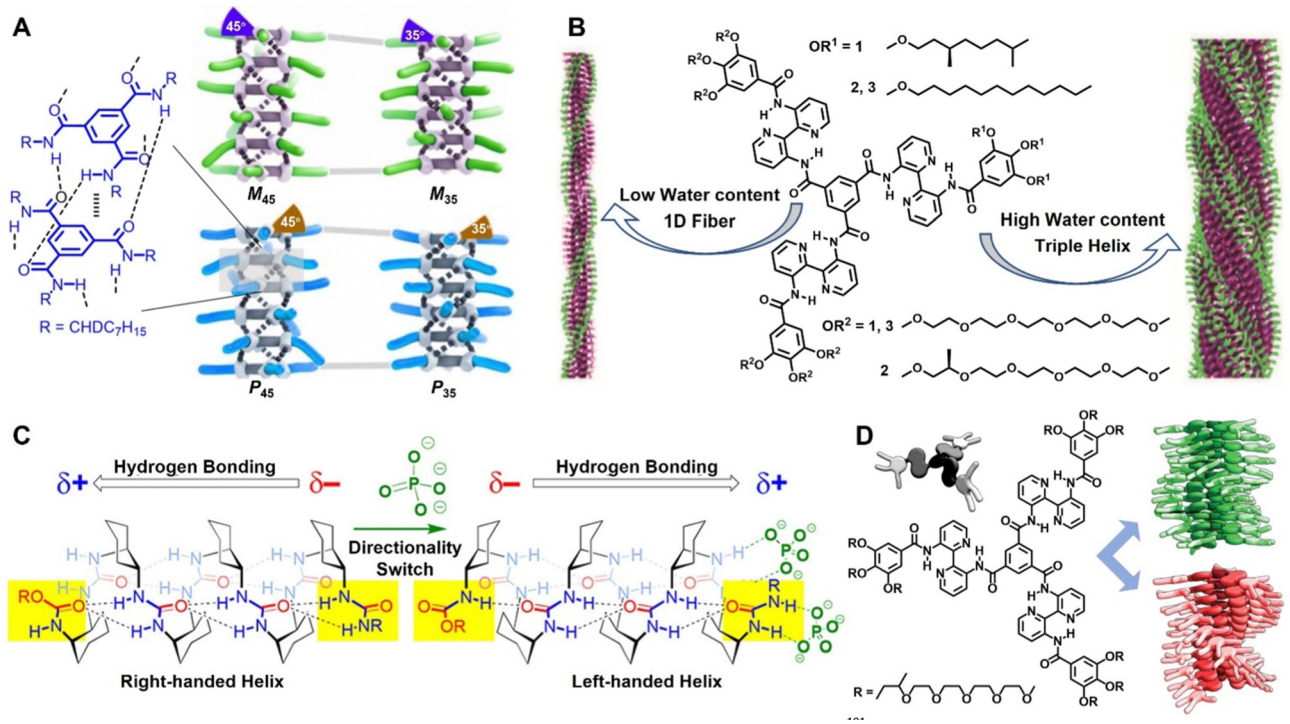

Fig. 10 (A) (*S,S,S*)-D-BTA conformations differing in helical sense (*P* or *M*) and dihedral angle θ (45° and 35°).[101] (B) Hierarchical self-assembly of amphiphilic BiPy–BTA discotics **1**–**3** (center), and supramolecular fiber (left) triple helical bundle by the solvent effect when water content increases.[105] (C) Molecular torsion balance of oligourea foldamers. Adapted from ref. 107, Copyright 2018, American Chemical Society. (D) BiPy-1 aggregation model with two competitive aggregation pathways.[109]

population of the two conformations. The foldamers exhibit a molecular torsion balance.

The final nanoscale morphology and the advanced properties of supramolecular materials are not only related to the basic building block structure, but also clearly related to the dynamics of the polymerization process.[108] Meijer *et al.*[109] addressed manifestations of pathway complexity and reported that the aggregation process of 1,3,5-benzenetricarboxamides (BiPy-1) in *n*-butanol is a competitive two-pathway mechanism, which refers to the processes of monomer nucleation and growth (Fig. 10D). The free monomer firstly aggregated in the cooling process into a disordered polymer and then continuous cooling makes the disordered polymer dissociate into monomers and form an ordered polymer.

2.7 Structure versatility of multiple hydrogen bonding building blocks

The development of non-covalently bonded supramolecular polymers has made great progress in recent decades,[36,110] but controllable synthesis of supramolecular polymers remains a challenge.[111] Normally, supramolecular polymers are achieved along two ways.[112,113] One is the traditional strategy involving assembly of covalently synthesized heterotopic monomers *via* non-covalent interactions. The other is supramolecular strategy in which non-covalently synthesized monomers also called supramonomers experienced traditional covalent polymerization (Fig. 11A).[114] Covalent polymerization of supramonomers makes the reaction process predictable and provides new perspectives for controllable synthesis of supramolecular polymers.[115] In addition, self-sorting is a self-assembly process based on reversible chemistry that forms complexes through selective recognition between specific monomers.[116,117] Linear supramolecular polymers were created by changing the rigidity of the bifunctional monomers in the self-sorting process and regulating their molecular weight.[118,119]

Zimmerman *et al.*[120] designed a module eDAN (Fig. 11B) that can be used for the reversible control of polymer networks. The weak binding between DeUG and the oxidized form was enhanced after reduction. Zhang *et al.*[121] integrated supramolecular chemistry and traditional interfacial polymerization, and introduced a controllable strategy, supramolecular interfacial polymerization, to construct supramolecular polymeric materials (Fig. 11C). $(UPy\text{-}SH)_2$ (oil soluble) involved in the thiol-maleimide click reaction and was polymerized with MA-C12 (water soluble) containing two maleimide at the water–chloroform interface. Amorphous supramolecular polymer films with a molecular weight of 68 kDa were formed, showing good thermal stability (238 °C, 5% weight loss). Compared with supramolecular polymerization in homogenous media, supramolecular interfacial polymerization is simple and controllable, which can be used with a variety of monomers, even if they are immiscible. Meanwhile, supramolecular polymers with high molecular weight can be fabricated unconfined to the mole ratio or concentration of the monomers.

Kinetically controlled living supramolecular polymerization (LSP) can control the length and dispersion of polymers.[122] George *et al.*[123] achieved structural and stereo co-control of supramolecular polymerization through implementing

Published on 03 January 2024. Downloaded by Yunnan University on 8/4/2025 1:35:41 AM.

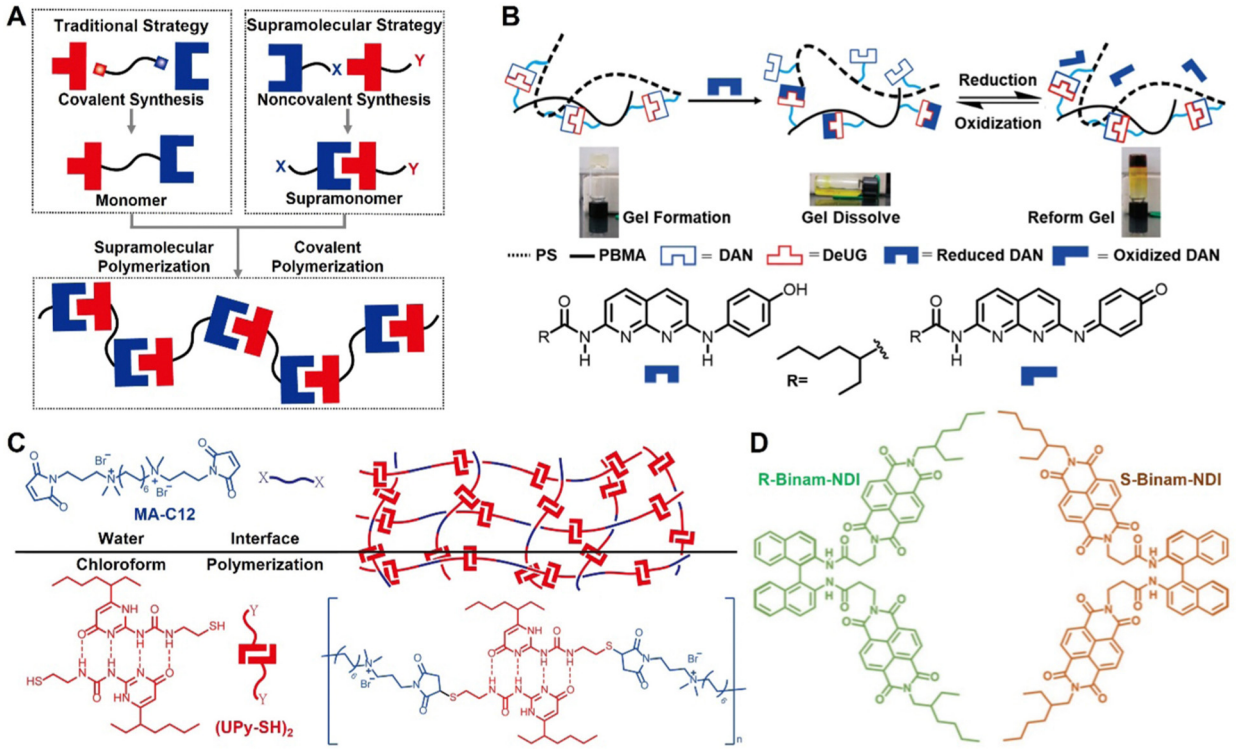

Fig. 11 (A) Comparison of the tradition strategy and the supramonomer strategy for fabricating supramolecular polymers.[112,113] (B) Schematic representation of hydrogen bonding facilitated redox.[120] (C) Supramolecular interfacial polymerization.[121] (D) Molecular structures of enantiomers *R*- and *S*-Binam-NDI.[123]

stereoselective seed-induced LSP. The enantiomers *R*- and *S*-Binam-NDI were synthesized by bischromophoric naphthalene diimide (NDI) and the chiral core (±)-1,1′-binaphthyl-2,2′-diamine (Fig. 11D).

Synergy of multiple non-covalent forces favors thermodynamically stable assemblies with predictable chemical transformation.[124,125] Hydrogen bonds narrow the distance between two reaction sites, enabling interacting sites spatially favorable in terms of position and orientation. Moreover, hydrogen bonds can activate the reaction sites and increase the effective concentration of the substrates. Kelly *et al.*[126] proposed a linear template for the reaction of two substrates assembled in a liquid phase (Fig. 12A). The template possessed two binding sites and interacted with two organic substrates simultaneously by triple hydrogen bonding, respectively. The reaction rate of the nucleophilic substitution reaction between the two organic substrates increased by 6 times. Two oligoamide strands were paired through hetero-complementary hydrogen bonding sequences, and then crosslinked into a macrocyclic structure followed by the introduction of *S*-trityl groups capable of forming reversible disulfide bonds with iodine (Fig. 12B).[127] The system showed high length-dependent selectivity, shorter strands possessing hydrogen bonding sequences that can be partially complementary to longer chains but not crosslinked. Complementary oligosamides have sequentially specific crosslinking in nonpolar solutions (methylene chloride) and competitive media (aqueous).

Tiefenbacher *et al.*[128] reported a large hexameric cage (Fig. 12C) based on intermolecular amido-amide dimerization. The organic cage had a cavity volume of ~2800 Å^3 and its structure was held together by 24 hydrogen bonds. It formed host–guest complexes with fullerenes (C_{60} and C_{70}) through favorable dispersion force and π–π interactions. The formation of the hexameric structure depended on concentration. Cyclotriveratrylenes (CTVs) are rigid concave cyclophanes,[129,130] and many aromatic units with CTVs show enhanced binding capacity because of the additional stacking between fullerenes and aromatic units.[131,132] Li *et al.*[129] developed CTV-based capsular structures by using C_3-symmertric CTV precursors to guide the aramido-derived foldamer segments to form three imine bonds *via* hydrogen bonding (Fig. 12D). The capsules form supramolecular host–guest systems with C_{60} and C_{70} in discrete solvents.

3. Multiple hydrogen bonding driven emerging supramolecular architectures

3.1 Chiral supramolecular assemblies

One advantage of supramolecular systems is that achiral molecules can be induced into chiral self-assembly. Chiral induction, also known as asymmetric induction, was proposed by Hermann Emil Fischer based on his work on carbohydrates.[133] The most common approach is to induce helical supramolecular assembly by chiral molecules.[134] The helical conformation of foldamers is dynamic in nature. Different helical conformations can be induced by non-covalent intermolecular bonding with chiral additives or by introducing chiral residues

 This journal is © The Royal Society of Chemistry 2024

Published on 03 January 2024. Downloaded by Yunnan University on 8/4/2025 1:35:41 AM.

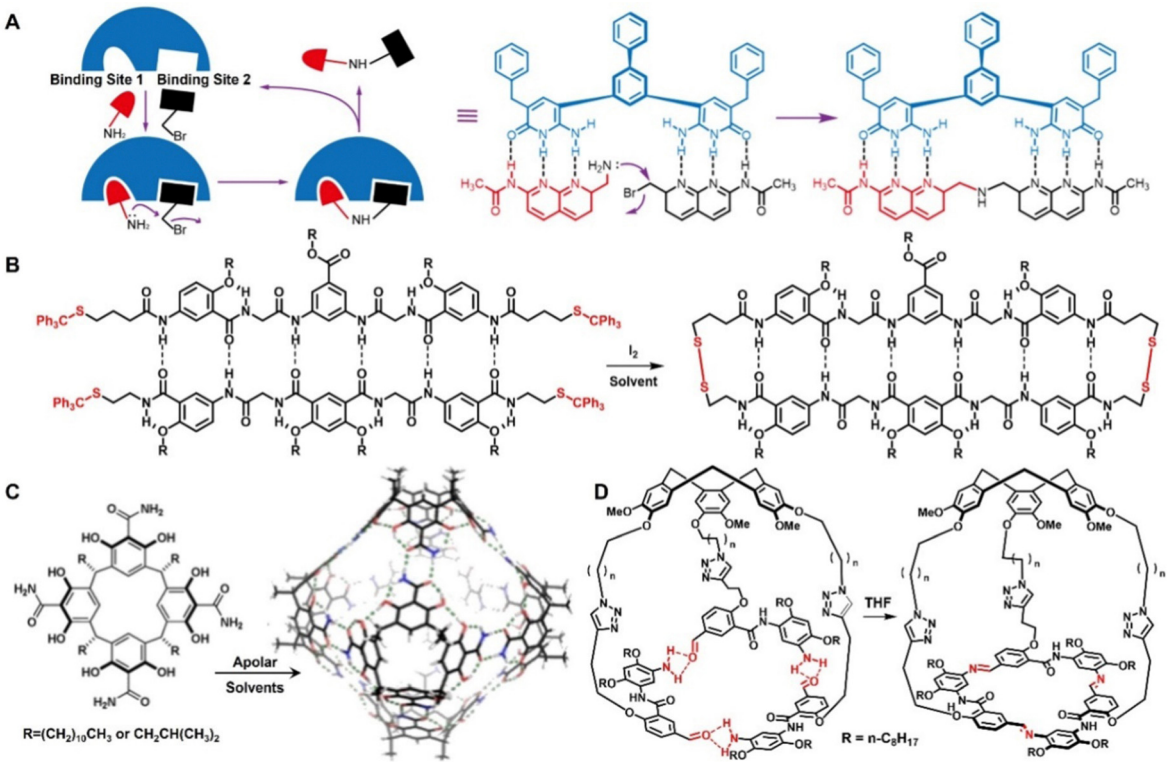

Fig. 12 (A) Two substrates binding with a template *via* triple hydrogen bonding.[126] (B) Molecular recognition *via* hydrogen bonding and the covalent crosslinking forming disulfide bonds.[127] (C) Hexameric hydrogen-bonded molecular cage.[128] (D) Capsule structure formed *via* hydrogen bonding directed self-assembly.[129]

at the chain end or pendant.[135] Their helical conformation changes depending on the solvent used.[136–138] Fig. 13A(a) shows chirality transfer between covalent/supramolecular polymers and small molecules.[139,140] Ishida *et al.*[139] designed the helical supramolecular polymers from dendritic carboxylic acid 1 (achiral) and amino alcohols (chiral, $X = 2^S/2^R$, $3^S/3^R$, $4^S/4^R \ldots$). The monomers form salt pairs $1{\cdot}X$ by electrostatic interaction, and then form a supramolecule through hydrogen bonding (Fig. 13A(b)). Copolymerization occurs when two salts with the same chirality are mixed, but not with oppositely chiral salts (Fig. 13A(c)). Because of this stereoselective copolymerization, helical supramolecular polymers can favour the enantiomeric composition of chiral amino alcohols. Xing *et al.*[141] realized the transformation of supramolecular chirality from supramolecular tilted chiral helical arrangement to nanoscale helical fibers. Amino acids provide chiral factors and grow in the 1D direction by hydrogen bonding with melamine. Octafluoronaphthalene and pyrene tune the wavelength of fluorescence emission by arene–perfluoroarene interaction.

Chiral amplification is a phenomenon in low molecular weight systems with helical supramolecular polymers and non-covalent bonds.[142,143] Green's group investigated the "sergeants and soldiers" principle[144,145] and the "majority-rules" effect that affect chiral amplification.[146] The principle of "sergeants and soldiers" is that a small number of chiral motifs (sergeants) manipulate the direction of many collective chiral motifs (soldiers). The "majority rule" effect is when a slight excess of one enantiomer relative to another creates potent helical sense that most enantiomers prefer. Ikai *et al.*[147] studied the polymerization of isocyanide **a** (Fig. 13B); the macromolecular components linked end-to-end by hydrogen bonding between amide chains. Based on "sergeant and soldier" effects, polymerization with 1 mol% chiral isocyanide **b**, 99 mol% achiral **a**, preferred-handed helix is formed based on dual intramolecular/intermolecular chiral amplifications.

Synthesis of enantiopure self-assembly from achiral components has been achieved using the "memory of chirality" (MOC),[148] through which enantiomerically enriched self-assembly can be preserved after the chirality inducer is replaced or removed by an achiral analogue while none of the components are chiral. Rebeck *et al.*[149] reported the assembly of symmetrical molecules *via* hydrogen bonding to form chiral molecular capsules with dissymmetrical cavities. This process involved hydrogen bonding donors on the terminal glycolurils and acceptors in the central bicyclic unit. The dimeric assembly was racemic due to an equal amount of two mirror-image forms in the presence of symmetrical guests. When the guests were chiral, these assemblies preferentially formed one of the two possible diastereomeric complexes. Yashima *et al.*[148] reported that optically active amines can induce macromolecular helicity. This helicity can be "memorized" when it was substituted with different achiral amines. While helicity was not maintained perfectly in the polymer, it can self-heal over time. Minor structural changes of achiral amines have significant effects on helicity retention efficiency.

Published on 03 January 2024. Downloaded by Yunnan University on 8/4/2025 1:35:41 AM.

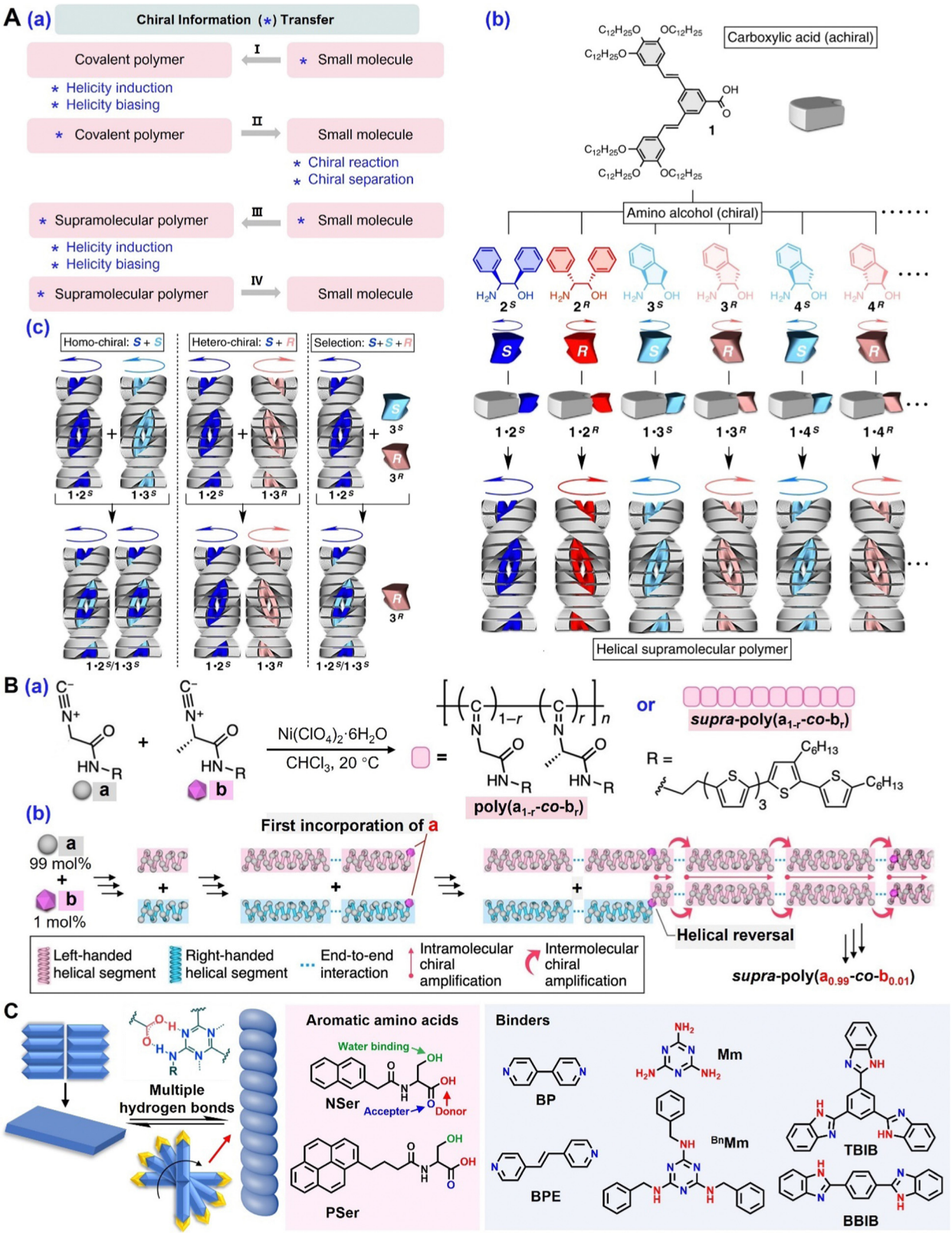

Fig. 13 (A) Schematic representations of (a) chirality transfer between covalent (I, II)/supramolecular (III, IV) polymers and small molecules, (b) helical supramolecular polymers prepared from achiral carboxylic acid and chiral amino alcohols, and (c) stereoselective copolymerization of two salts.[139] Reproduced under the terms of the CC–BY Creative Commons Attribution 4.0 International License (https://creativecommons.org/licenses/by/4.0/). (B) Chiral amplification of preferred-handed helical formation. (a) Polymerization of **2** and **1L**, and (b) chiral amplification according to "sergeants and soldiers" effects. Adapted from ref. 147, Copyright 2019, American Chemical Society. (C) Controlling chiral nanostructures through hydrogen bonding among amino acids and pyridine-based binders.[157]

 This journal is © The Royal Society of Chemistry 2024

Published on 03 January 2024. Downloaded by Yunnan University on 8/4/2025 1:35:41 AM.

In most cases, the induction and modulation of supramolecular chirality require the presence of intrinsic chirality components, including the assembly molecules themselves, chiral co-assemblies or chiral dopants. In fact, supramolecular chirality or macroscopic chirality can be achieved with achiral molecules.[150] Controlling the chirality of functional supramolecules in self-assembled systems is essential for possible applications in enantioselective catalysis mimicking the catalytic activity of enzymes, molecular recognition or materials science.[151–154] The enantioselective non-covalent synthesis of enantiomerically pure self-assembled structures is crucially challenging, because these assemblies possess low kinetic stability. Wei *et al.*[155] prepared chiral twisted nanoribbons of achiral oliganiline derivatives $C_{24}H_{20}O_3N_4$ by chemical oxidation of aniline in solvents (alcohol and water). π–π stacking and hydrogen bonding are the driving forces for twisted nanoribbon formation, which are controlled by ethanol content in the solvent. Zhang *et al.*[156] studied the chiral generation of a binary charge transfer complex from achiral components. The complex has C–H···N torsional backbone hydrogen bonds, lattice strain of torsional receptor and solvent–solute induces symmetry-breaking interactions, allowing metastable achiral groups to spontaneously pass through simple solutions (polar solvents) assembled to form helical aggregates. Zhao *et al.*[157] reported that N-terminal aromatic amino acids can assemble into lamellar microsheets, which molecularly stack on the 2D direction and therefore devoid of chirality. The introduction of achiral pyridine-based binders can bind to these aromatic amino acids by hydrogen bonding to assemble chiral nanostructures (Fig. 13C).

Supramolecular assemblies with chiral structures show attractive and promising application value as novel chiral materials in chemistry and nanotechnology, such as chiral recognition, chiral optical switching, asymmetric catalysis, and circular polarization luminescence.

3.2 Multiple hydrogen bonding module as a stimuli responsive source

Hydrogen bonds with high strength and good reversibility are ideal non-covalent bonds employed in constructing supramolecular polymers.[158,159] The systems generate macroscopic responses based on changes in the molecular architecture of materials induced by an external environment (temperature, light, chemical, stress, redox, and ultrasound).[37,160–165] Hydrogen bonding helps supramolecular polymers achieve intriguing properties, self-healing,[166,167] folding,[168] mechanochemistry,[169] and shape memory.[170–174]

A UPy motif possesses high dimerization constant, exceptional bonding energy and dynamic nature, promoting the development of stimuli responsive supramolecular polymers.[175–177] Weder *et al.*[178] prepared a light and temperature-responsive supramolecular polymer adhesive by introducing UPy motifs into copolymers provided by poly(alkyl methacrylate)s. Materials can be rebonded or de-bonded with light or heat. The supramolecular crosslinks formed by UPy dimerization significantly improved the adhesion in the rubbery state, and permit good adhesion over a wide temperature range. Linear supramolecular polymers prepared by Tang *et al.* were self-assembled from *E*-isomers containing azobenzene with UPy motifs.[179] The *E*-isomer was transformed into the *Z*-isomer under UV irradiation, which can form supramolecular polymers as well (Fig. 14A). Reversible *trans*/*cis*-isomerization of supramolecular polymers was achieved under the alternating irradiation of visible and UV light. The siloxane oligomers $(UP)_3T$ synthesized by Yao *et al.*[180] formed 3D networks with UPy dimers, which are further assembled into larger highly crystalline stacks (Fig. 14B). The material showed water-enhanced healing properties, enabling ambient water molecules to facilitate the dissociation of polyvalent hydrogen bonds *via* the gas permeable siloxane network for efficient and rapid healing (70 °C, 5 minutes, strength recovery 98%). Anthamatten *et al.*[158] obtained biocompatible soft materials by integrating UPy into linear and crosslinked polydimethylsiloxane using a hydrosilylation reaction. Macromolecular structures with tight side substituents avoid the stacking of hydrogen bonding moieties. The obtained siloxane network features the presence of both thermoreversible crosslinks and covalent crosslinks. Yan *et al.*[181] reported a supramolecular polymer material imitating the impact resistance of sea cucumber dermis. The aromatic structure of UPy predisposes the dimers to fibrous assembly, which can further enhance the soft polymer network.

Changing the concentration of the crosslinker can tune the degree of crosslinking in the hydrogen bonding based polymer network, resulting in the preparation of tailor-made materials. Weck *et al.*[182] prepared terpolymers containing metal coordination sites and hydrogen bonds using ring-opening metathesis polymerization (Fig. 15). The addition of two corresponding complementary modules or crosslinkers caused crosslinking *via* cyanuric acid groups and the activated SCS pincer Pd centers. The network formed using both crosslinkers was stronger (higher dynamic modulus) than the network formed using one crosslinker. Hydrogen bonding and metal-coordination crosslinking networks endow polymers with thermally reversible and chemically responsive behavior, respectively. Lin *et al.*[183] synthesized a conductive self-healable gel supramolecular network in which hydrogen bonds, ionic bonds, and coordinate bonds form reversible non-covalent networks, providing injectable conductive self-healable gels. The gels are highly stretchable (>5000%) and ultra-fast self-healable (restore mechanical performance in 90 s, restore 95% electrical performance in 0.7 s). Huang *et al.*[184] synthesized supramolecular gels with polystyrene (PS) and poly(butyl methacrylate) (PBMA) *via* host–guest interactions and quadruple hydrogen bonding. eDAN destroyed the DAN·DeUG network, causing the supramolecular gels to swell. However, the oxidized eDAN cannot compete with the DAN unit, and DAN·DeUG was re-formed, accompanied by gel shrinkage. After reduction of oxidized eDAN, the gel expanded again. The gel was ion-responsive because of the host–guest interactions. K^+ and Cl^- disassembled the host–guest interactions. After the addition of 18-crown-6 and Ag^+, respectively, the threaded structure was recovered, resulting in a change in the gel volume. The size of the gel can be regulated by a competitive guest or a counterion. This supramolecular gel can mimic muscles and can be used in the design of biomaterials.

Published on 03 January 2024. Downloaded by Yunnan University on 8/4/2025 1:35:41 AM.

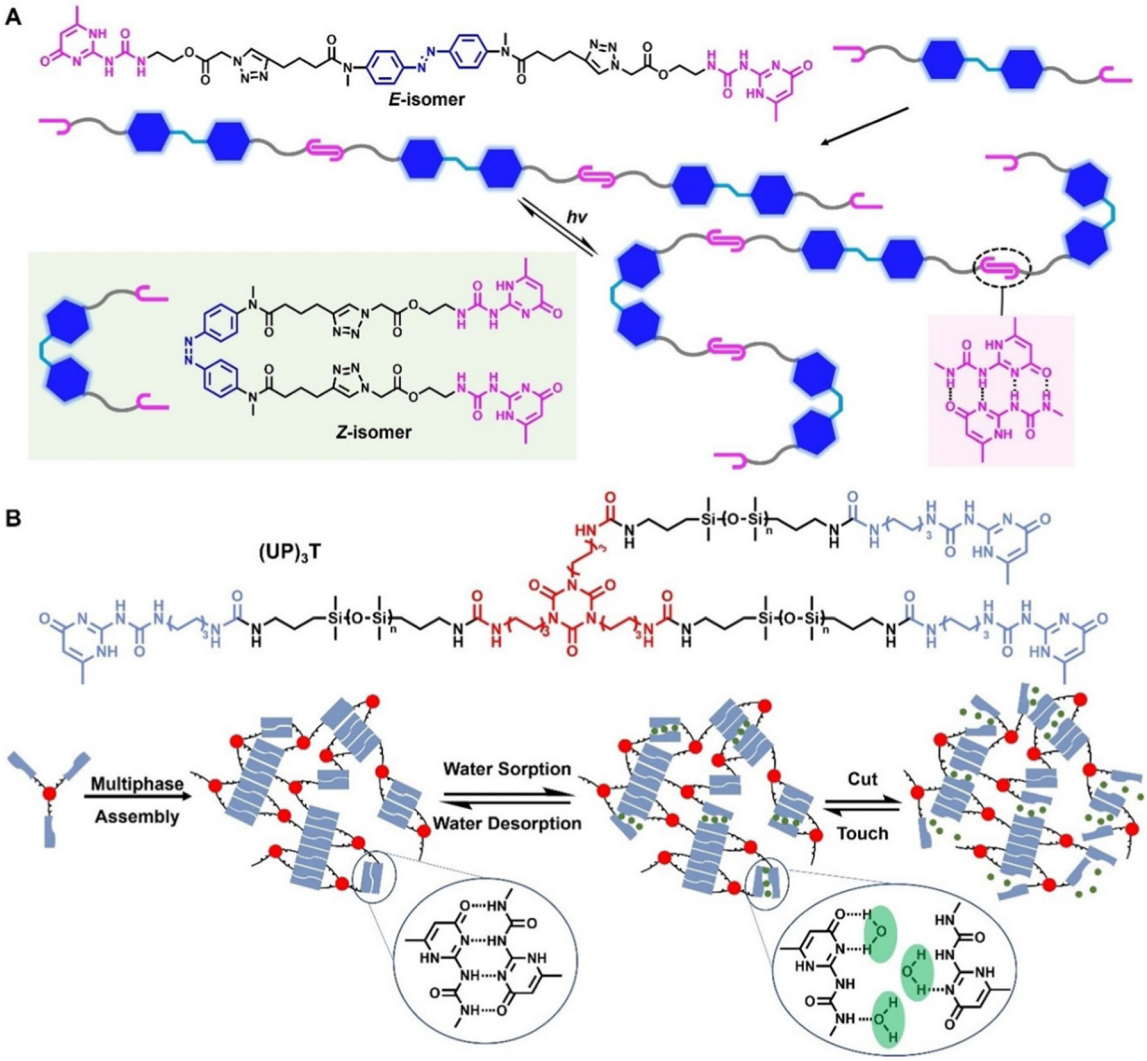

Fig. 14 (A) Supramolecular assembly processes of *E*- and *Z*-isomers containing azobenzene and UPy.[179] (B) Self-assembly of $(UP)_3T$ units into 3D networks and dissociation of UPy dimers with water molecules.[180]

3.3 Multiple hydrogen bonding for interpenetrating polymer networks

Polymer blends are superior to individual components and can have multiple functions, such as good mechanical properties, biodegradability, and low cost, and enable wider applications of polymer materials.[185] Most polymer blends are immiscible due to a high polymerization degree. Therefore, it is very important to reduce the interfacial energy and phase separation propensity. An interpenetrating polymer network (IPN) is a polymer blend composed of two or more polymer networks that are individually crosslinked and interpenetrating.[186] Miscible properties are obtained by introducing IPNs into polymer blends, which are supposed to be nearly a single-phase structure. In addition, monomers with weak hydrogen bonds (amino, hydroxyl, carboxyl, and pyridyl) are also used to improve the compatibility of blends.[187,188] IPNs can be generated through reversible crosslinking between and within polymer chains through homo- or hetero-hydrogen bonding units.[189,190] Tang *et al.*[191] created physical

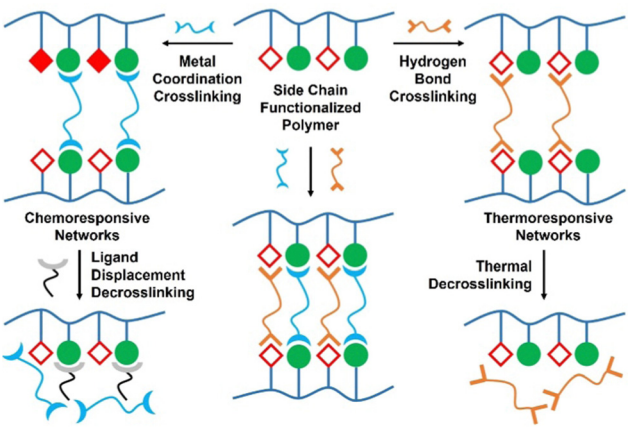

Fig. 15 Terpolymers containing metal coordination sites and hydrogen bonds ensuing multi-responsiveness.[182]

 This journal is © The Royal Society of Chemistry 2024

Published on 03 January 2024. Downloaded by Yunnan University on 8/4/2025 1:35:41 AM.

crosslinks and entanglements for polymers with pendant fatty chains (Fig. 16A). Hydrogen bonding between poly(4-vinylpyridine) (P4VP) and acid-containing copolymers created physical crosslinking and further wrapped around them with P4VP chains. The mechanical strength and toughness of bio-based polymers are improved by hydrogen bonding and chain entanglement.

Multiple hydrogen bonding units with high fidelity and affinity can be used to prepare polymer blends.[72,75] Konkolewicz *et al.*[192] reported an IPN material in which the first network was crosslinked with UPy and the second network was crosslinked with a furan-maleimide Diels–Alder adduct (FMI) (Fig. 16B). IPNs outperformed the single network composed of FMI and UPy crosslinkers in terms of mechanical properties, self-healing, and malleability. Zeng *et al.*[193] developed a conductive polymer hydrogel consisting of a supramolecular network of negatively charged poly(4-styrene sulfonate) crosslinked by UPy groups to form an interpenetrating conductive network, and electrostatic interactions with PSS chains occurred (Fig. 16C). Hydrogen bonds endow hydrogels with stretchable and self-healing properties. Ion transport assists electron conduction, enabling the hydrogel to exhibit excellent electrical conductivity and high sensitivity to external strain. Li *et al.*[194] introduced puerarin into chitosan physical crosslinking hydrogels to prepare IPN composite hydrogels, and their storage modulus and loss modulus were increased by 3 orders of magnitude. The amino groups of chitosan formed hydrogen bonding with puerarin hydroxyl groups, and the molecular chains of chitosan and the nanofibers of puerarin were intertwined, making the network structure of the composite hydrogel denser. The hydroxy group of puerarin forms hydrogen bonds with the amino group of chitosan, and the nanofibers of puerarin intertwine with the molecular chain of chitosan, which makes the network structure of the composite hydrogel denser.

Multiple hydrogen bonding is an emerging and efficient strategy for IPNs. The resultant blends *via* highly stable hetero- or homo-pairing units can overcome the repulsive force between polymers to form reversible supramolecular networks.[195] This method is currently limited to certain polymer pairs and requires large amounts of comonomers to induce miscibility.[196] It presents a method for developing new polymers using the dynamic reversible multiple hydrogen bonding interactions as building blocks.

3.4 Multiple hydrogen bonding assisted organic frameworks

Hydrogen bonded organic frames (HOFs) are crystalline porous materials, generally composed of organic or metal–organic building units interlinked by intermolecular hydrogen bonds.[197,198] Compared with covalent organic frameworks (COFs) and metal–organic frameworks (MOFs), HOFs possess characteristics of mild synthesis conditions, high crystallinity, solvent processing, easy repair, and regeneration.[38,199] Stable and porous HOFs are prepared by properly selecting rigid building units with specific geometric configurations and introducing other forces, such as interpenetration or π–π interaction and electrostatic interaction.[200,201] Several hydrogen bonding motifs, such as carboxylic acid, pyridine, and imidazole, have been used to construct porous HOFs.[199,202,203]

Two dihydropyridyl products **L1** and **L2** were prepared by Schröder *et al.* (Fig. 17A).[90] **L1** assembled a porous organic framework [**L1**]·2.5DMF·3MeOH (**SOF-1**) with pyridyl-modified channels by hydrogen bonding and π–π stacking. It has permanent pores, exhibits excellent thermal stability and gas absorption capacity. **SOF-1** can be used to purify C_2H_2 and natural gas and can remove carbon dioxide from the air. Under the crystallization conditions of **L1**, the analogue **L2** formed two solvates of pale yellow tablet and block without a 3D network structure. Chen *et al.*[204] prepared HOFs with larger surface area

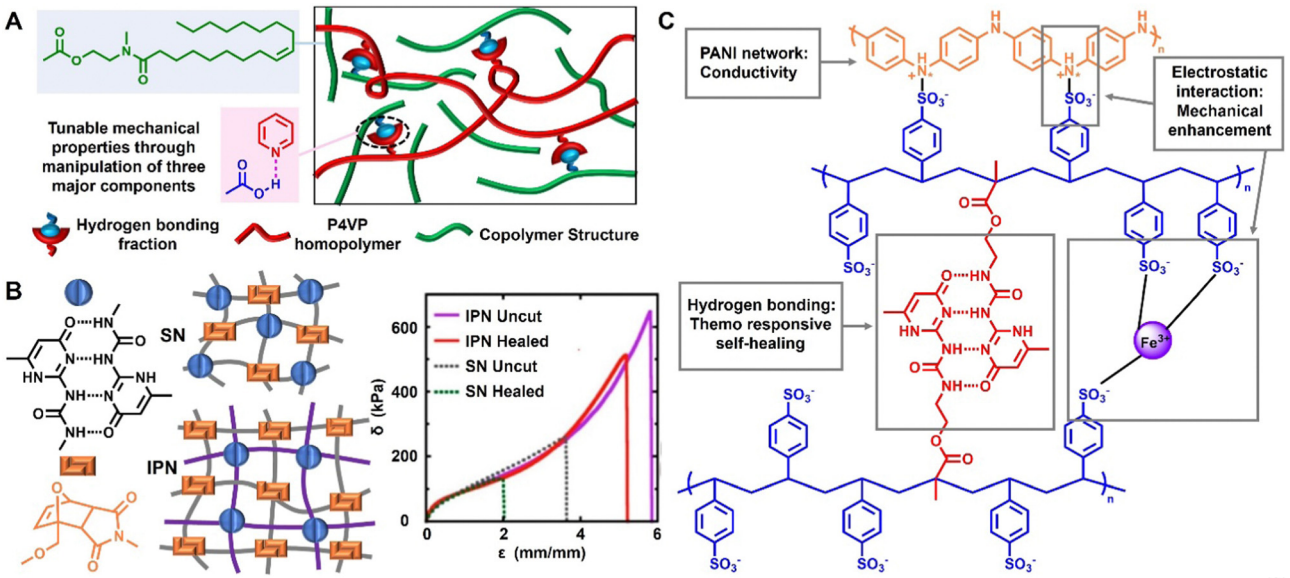

Fig. 16 (A) P4VP interacts and wraps oil-based copolymers, producing physical crosslinking toward more efficient supramolecular chain entanglements.[191] (B) IPN and single network with UPy and FMI linkers.[192] (C) Schematic structure of supramolecular conductive PANI/PSS-UPy hydrogels.[193]

Published on 03 January 2024. Downloaded by Yunnan University on 8/4/2025 1:35:41 AM.

(2573 $m^2 g^{-1}$) and pore size (pore volume 1.36 $cm^3 g^{-1}$) using organic building units of 6,6′,6″,6‴-(pyrene-1,3,6,8-tetrayl)tetrakis(2-naphthoic acid). π–π stacking and hydrogen bonding in HOFs endow them with excellent thermal and chemical stability. After soaking in strong acid, strong alkali, and boiling water, HOFs retained their crystallinity. The HOFs can effectively separate CH_4 from C_3 and C_2 hydrocarbons.

Zhang *et al.*[205] assembled flexible porous HOF 8PN with permanent porosity (Fig. 17B). Nine crystal conformations were obtained based on different stimuli, such as guest, temperature, and pressure. The void space varies from 89.4 $Å^3$ to 1816.0 $Å^3$. Under the external stimulation, the multimode reversible structure transformations of HOF 8PN were realized with the change of luminescence characteristics. Adjusting the molecular conformation and assembly of HOF 8PN building blocks can be adapted to guests of different aggregation states, sizes, and shapes, resulting in high-quality co-crystals. Stoddart *et al.*[206] prepared two 3D interpenetrating isomers of HOFs by changing the crystallization conditions. PETHOF-1 is composed of two separate networks connected symmetrically in reverse, forming an interwoven topology. However, PETHOF-2 is composed of five individual networks that are related to each other by specific symmetry and packed in an alternating fashion. After desolvation, the two approaches produced microporous superstructures with surface areas of over 1100 $m^2 g^{-1}$.

3.5 Multiple hydrogen bonding supramolecular adhesives

Hydrogen bonding affects the mechanical properties and macroscopic adhesion behavior of a supramolecular polymer and its dynamic association/dissociation can achieve energy dissipation in materials. Zimmerman *et al.*[207] reported supramolecular coupling agents based on units DAN–DeUG ($K_a = 2 \times 10^8$ M^{-1} in $CHCl_3$) (Fig. 18A). These quadruple hydrogen bonding units have been used for functional modification of material surfaces.[72,208,209] The DAN–DeUG interaction is consistent with the mechanical properties of the supramolecular adhesive. Non-specific adhesion occurs when urea-based supramolecules are attached to the surface of the material.[210] The fluoroalkyl surface maximizes DeUG–DAN interaction and minimizes nonspecific adhesion. Films prepared using monoalkoxy silane have larger contact angles, thicker film layers, and weaker adhesion than those prepared with trialkoxy silane. Zhu *et al.*[91] reported a supramolecular hydrogen bonding adhesive (Fig. 18B) with shear strength greater than 12 MPa. The heterocomplementary barbiturate (Ba) and Hamilton wedge (HW) moieties interact to produce hydrogen bonding supramolecular polymer networks. Ba or HW units adhere firmly to the substrate through hydrogen bonding interactions. The supramolecular adhesion to the glass can bear 10.8 kg.

Gao *et al.*[211] designed an intelligent adhesive hydrogel based on adenine and thymine, which were distributed in a pure

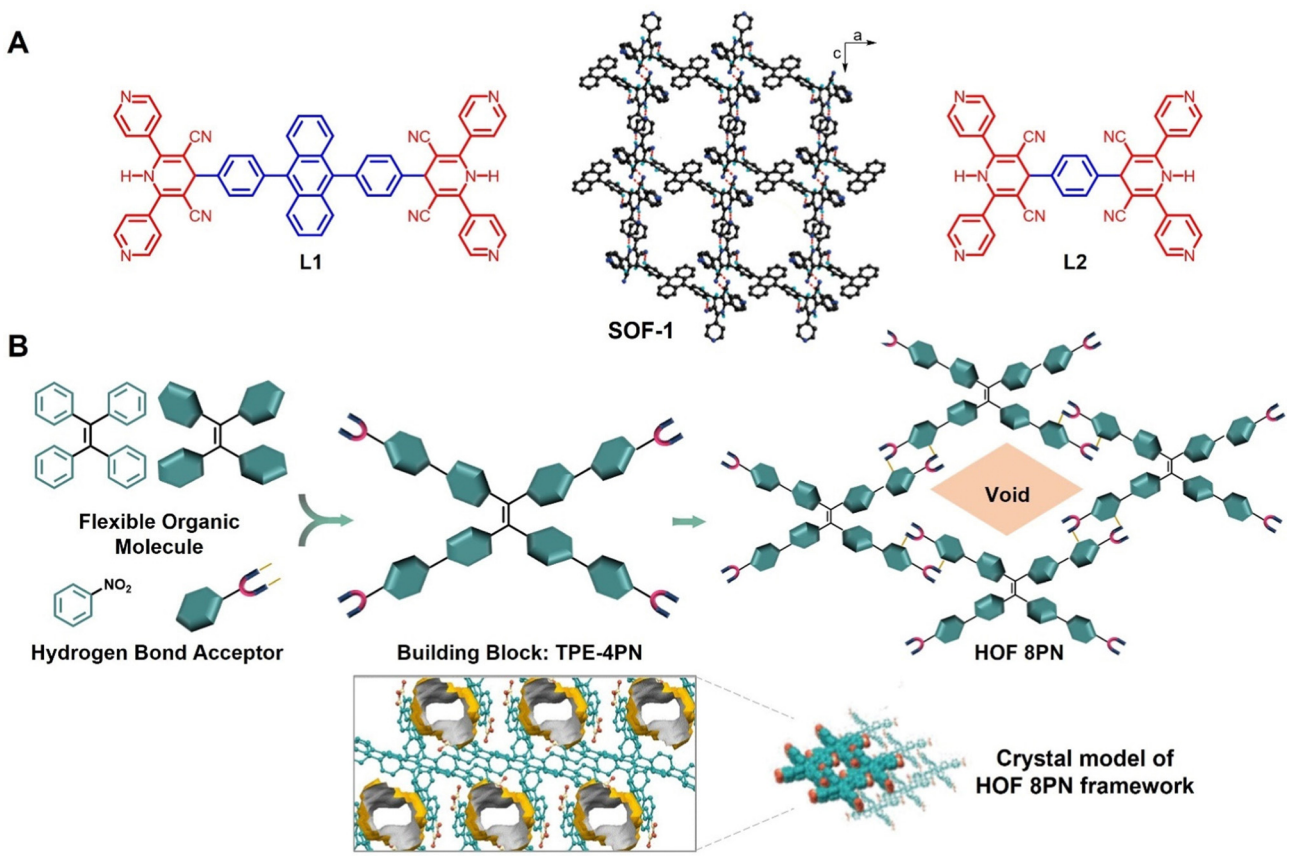

Fig. 17 (A) Molecular structures of **L1** and **L2**, and the nanochannel of SOF-1, the red dashed lines are hydrogen bonds.[90] (B) Schematic representation of HOF 8PN from TPE-4PN.[205]

 This journal is © The Royal Society of Chemistry 2024

Published on 03 January 2024. Downloaded by Yunnan University on 8/4/2025 1:35:41 AM.

acrylamide hydrogel as adhesion groups. Hydrogen bonding, metal complexation, and hydrophobicity are the forces responsible for the hydrogel's adhesion. The maximum peeling strength of the hydrogel on an aluminum surface was 330 N m^{-1}. After repeated peeling tests for more than 30 times, the adhesive properties were still strong.

Supramolecular adhesives can be used in some special environments. Sun *et al.*[212] prepared a durable atomic oxygen-resistant coating for low Earth orbit (LEO) space with self-healing properties. The coating is a 3D supramolecular polymer formed by hydrogen bonding of UPy-functionalized polyhedral oligomeric silsesquioxane. The coating can quickly repair mechanical damage sustained at 80 °C or LEO space, restoring its atomic oxygen-resistant function. Dong *et al.*[213] prepared supramolecular adhesives by hydrogen bonding interactions between water and pillar[5]arene-crown ether. The adhesive showed high adhesive strength (1.17 MPa) to metallic materials in liquid nitrogen at −196 °C.

3.6 Multiple hydrogen bonding modules as energy dissipators

The strength of hydrogen bonding has important influence on the viscoelasticity of supramolecular polymers.[214] The bond energy of hydrogen bonding is about 25–30 kJ mol^{-1},[215] which is responsive to external stimuli like mechanical stress, light, and heat. It can be applied to the research and development of smart materials.

Zhang *et al.*[5] proposed that DAN–DeUG/UPy/UG functionalized materials could be used as energy dissipators (Fig. 19A). Entangled polymer chains are cross-linked within and between polymer chains by hydrogen bonding interactions. Multiple hydrogen bonding modules provide additional energy dissipation sources when stretching interlocking polymer chains and rupturing hydrogen bonding pairs.

Efficient energy dissipation structures and homogeneous networks are the key factors to fabricate high stiffness and toughness polymer materials. Energy dissipative networks containing sacrificial bonds (hydrogen bonding, electrostatic interactions, and metal–ligand coordination) generally have high toughness; however their stiffness is low due to the inherently weak nature of these interactions. This problem can be solved by introducing multiple hydrogen bonding systems into the polymer, which form stronger intrachain and bonding interactions and increase the ability to dissipate energy. Liu *et al.*[216] developed nucleobase-functionalized homopolymers by thiol–ene polymerization (Fig. 19B). The intermolecular and intramolecular hydrogen bonding interactions of the homopolymer mixture makes it have better damping capacity and energy dissipation. Its toughness and adhesive strength were 73.8 MJ m^{-3} and 16.2 MPa, respectively. Creton *et al.*[217] obtained biurea-functionalized polyisobutenes (PIBUT) with low molecular weight through the reaction of 2,4-toluene diisocyanate and polyisobutene (PIB). The introduction of biureas formed supramolecular hydrogen bonds, which enabled the ordered self-assembly of the polymer materials at room temperature. At 80 °C, PIBUT behaved as a highly viscoelastic fluid, and annealing restored its ordered structure. PIBUT was highly dissipative when deformed and exhibited good adhesion on steel and silicone surfaces.

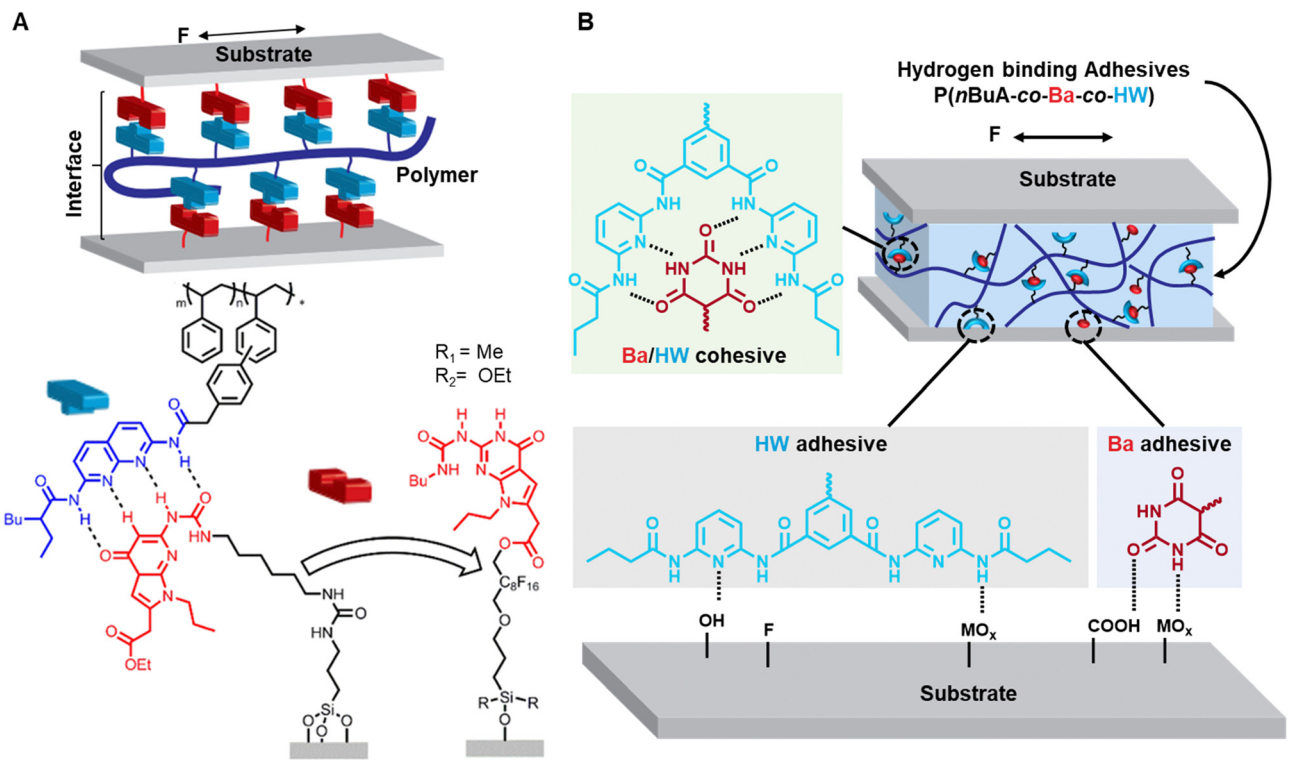

Fig. 18 (A) Hydrogen bonding adhesive based on units DAN–DeUG.[207] (B) Interfacial gluing between P(*n*BuA-*co*-Ba-*co*-HW) and the substrate *via* hydrogen bonding.[91]

Published on 03 January 2024. Downloaded by Yunnan University on 8/4/2025 1:35:41 AM.

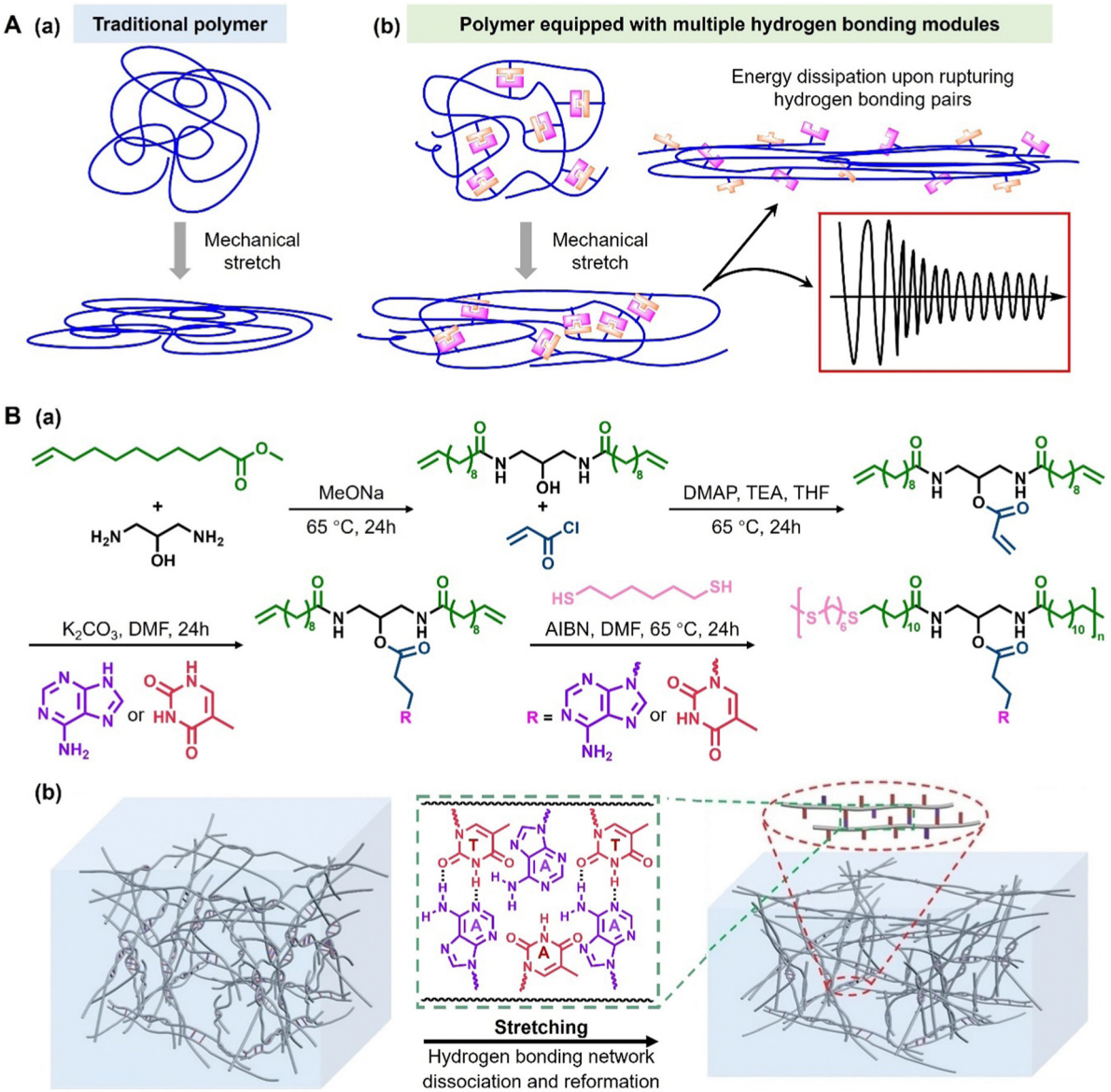

Fig. 19 (A) Schematic representations of (a) conventional polymers and (b) supermolecule polymers equipped with multiple hydrogen bonding modules responding to mechanical forces by stretching chains.[5] (B) (a) Syntheses of nucleobase-functionalized homopolymers by thiol–ene polymerization and (b) schematic representations of a hydrogen bonding network of the copolymers.[216]

3.7 Quantitative analysis of nano-adhesion

In advanced functional material design, quantitative analysis of multiple hydrogen bonding interactions is of great significance to understand the structure–property relationship. Studying the interactions of multiple hydrogen bonding in a material matrix is a challenge because the various non-covalent interactions are related. It is important to directly measure the forces between multiple hydrogen bonds,[218–220] and atomic force microscopy (AFM) is applied not only to provide images on an atomic scale,[221,222] but also to study the interactions between single strands of DNA[223] as well as other aspects.[47,224,225] Gaub was a pioneer in using AFM to measure the interaction forces of single molecules. The adhesion of biotinylated agarose bead was measured using an avidin functionalized AFM tip (Fig. 20A).[47] During force scans, the deflection of the cantilever approaching and retreating from the bead was recorded and was converted into force by the measured cantilever spring constant. Avidin blocked most of the biotin on the agarose bead, and the unbinding force of single molecular pairs was detected to be 160 ± 20 pN, and the adhesion force was an integer multiple of that. Single molecular force spectroscopy (SMFS) based on AFM can explore molecular recognition interactions at the single molecular level, and obtain quantitative data on macromolecular bond rupture force and molecular stretching behavior.[34] Gaub *et al.*[226] measured base pairing forces of nucleotides using SMFS. When double-strand DNA was overstretched, the resulting single strands paired into hairpins because the bases complement each other (Fig. 20B). The

 This journal is © The Royal Society of Chemistry 2024

Published on 03 January 2024. Downloaded by Yunnan University on 8/4/2025 1:35:41 AM.

unzipping of these hairpins indicated that the unbinding forces of the base pair of A–T and G–C were 9 ± 3 pN and 20 ± 3 pN.

Quadruple hydrogen bonding interactions in poly(ethylene glycol) (PEG)-linked UPy polymers were studied by SMFS between the Au-coated AFM tip and PEG–UPy immobilized on the Au substrate (Fig. 20C).[218] PEG decoupled the complexation process from the surface, enabling calculation of single-molecule bond-rupture,[227] thus directly determining the exact force of single UPy–UPy complex rupture. There is a logarithmic relationship between the rupture forces and loading rates at 301 K, but no dependence at 330 K. This was predicted by Evans *et al.*[228,229] and confirmed by several studies.[230–232] The rupture force of the single UPy–UPy complex in hexadecane was measured as 180 ± 21 pN.[220] The rupture force of the supramolecular polymer chain decreased with the increase of stretching length (Fig. 20D). However, the rupture force of a single complex decreased with the increase of spacer length and consecutive bond number.[229,233–235]

Zhang *et al.*[215] studied the interactions of quadruple hydrogen bonding under mechanical stress using DAN modified polystyrene, DeUG modified polybutyl methacrylate (PBMA–DEUG) and UPy modified polybutyl methacrylate (PBA–UPy) as adhesive agents by measuring the adhesion force (Fig. 20E). The maximum load at failure showed quadruple hydrogen bonding interactions contributed significantly (72%) to the total adhesive force. For quadruple hydrogen bonding modified glass surfaces, their pairing efficiency was greatly improved using polymers modified by complementary quadruple hydrogen bonding partners, with the DAN–DeUG pairing efficiency of up to 40%. The rupture force of UPy–UPy was 160 pN, and that of DAN–DeUG was 193 pN. Detecting single pairs of rupture forces of quadruple hydrogen bonding motifs through nano-adhesion measurements is helpful to understand its recognition behavior at material surfaces and interfaces.

4. Multiple hydrogen bonding stimulated supramolecular architectures in biomedical application

In biological system and biomedicine area, nano-adhesion is an important force at the molecular level which is associated with

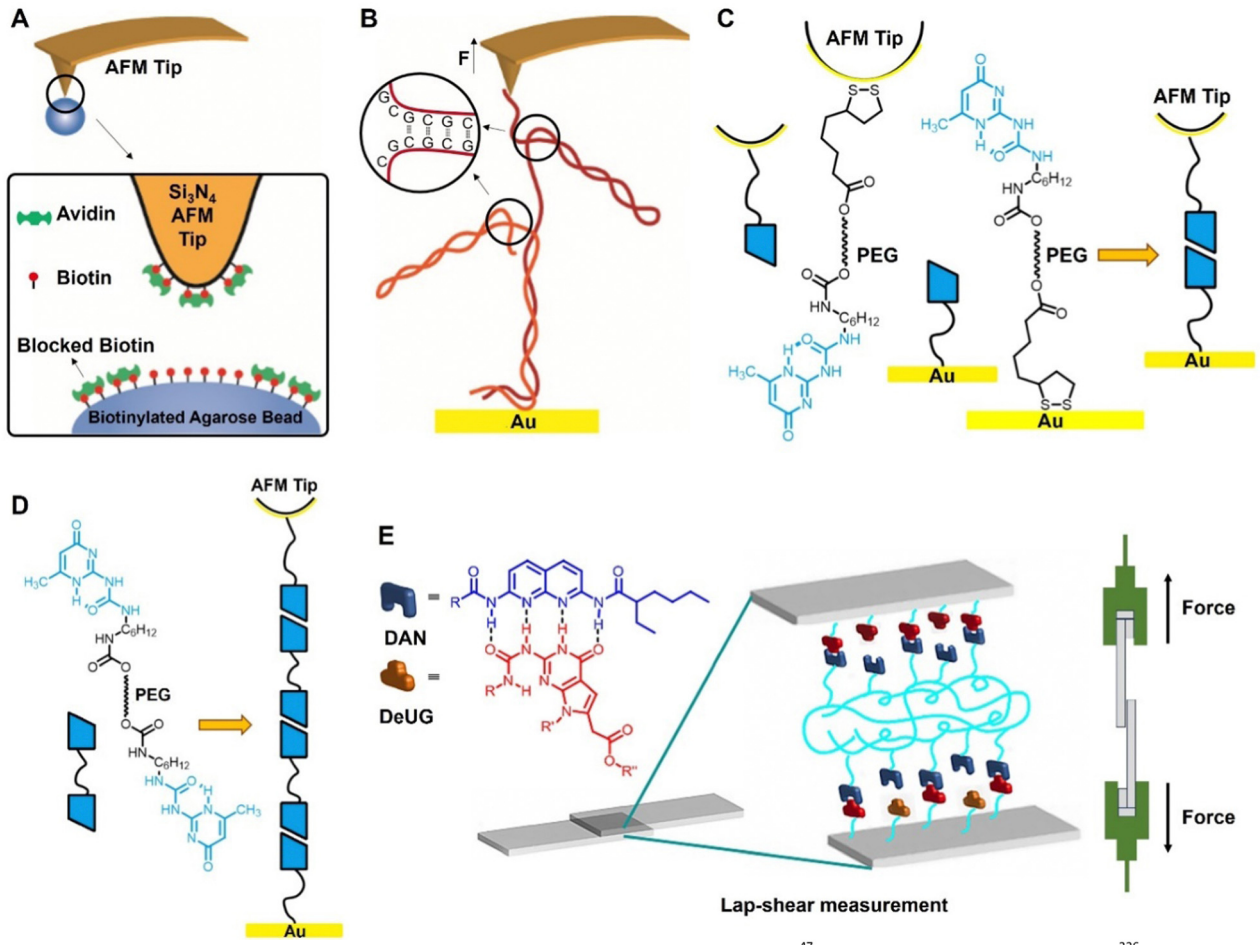

Fig. 20 (A) Avidin functionalized AFM tip measured the base pairing power of biotinylated agarose bead.[47] (B) Two strands of DNA form hairpins.[226] (C) PEG–UPy disulfide self-assembled into quadruple hydrogen bonding dimers.[218] (D) Single supramolecular polymer chain, Adapted from ref. 220, Copyright 2005, Wiley-VCH Verlag GmbH & Co. KGaA, Weinheim. (E) Testing rupture force of single pairs DAN–DeUG.[215]

Published on 03 January 2024. Downloaded by Yunnan University on 8/4/2025 1:35:41 AM.

the molecular recognition process for signal transduction, cell–cell adhesion and proliferation. It is vitally important for elucidating the working mechanism and diagnosis of different diseases. Biomedical applications often require specific functions, such as biocompatibility, aqueous compatibility, biodegradability, stimulus responsiveness and biological activity.[236,237]

4.1 Unique drug design evolution for myotonic dystrophy

Myotonic dystrophy (DM) is an autosomal dominant genetic disease affecting multiple organs. It is characterized by progressive myasthenia, endocrine disorders, muscular atrophy and myotonia.[238] DM1 is derived by abnormal expression of cytosine-thymine-guanine (CTG) repeats (dCTG or CTG^{exp}, >50–2000) in the 3′-untranslated region of *DMPK* gene on chromosome 19.[239,240] CTG repeats, along with the corresponding expanded transcripts r(CUG), have large amounts of weakly paired T–T/U–U mismatch. The r(CUG) complexes sequester muscleblind-like (MBNL) proteins that should be involved in RNA splicing, editing, and translation. In comparison to DM1, myotonic dystrophy type 2 (DM2) is rarer and has relatively mild symptoms. DM2 is associated with abnormal expansion of cytosine-cytosine-thymine-guanosine (CCTG) repeats (75–11 000) in intron 1 of the zinc finger protein gene (ZNF9) on chromosome 3. Then at the RNA level, transcribed CCUG repeat, r(CCUG), also sequesters muscleblind-like protein 1 (MBNL1) and thus induces DM2. It has been suggested that the high affinity unit is selective for T–T/U–U mismatches in the CTG and CUG repeats and can reverse as the phenotype through inhibiting the MBNL1 protein from binding, thus allowing mRNAs and the protein to function normally (Fig. 21).[241]

Although $\mathbf{D_1}$ strongly binds to CCTG-containing DNA, it does not recognize CCUG repeats and therefore cannot inhibit the binding of MBNL1 to $(CCUG)_6$. Ligands $\mathbf{D_2}$ and $\mathbf{D_3}$ (Fig. 22C) exhibit good selectivity for CCUG.[242] $\mathbf{D_1}$ is active *in vitro* and is a potent inhibitor of $(CUG)_{12}$·MBNL1 interaction. However, it was not active in the DM1 cellular model, due to the low solubility in water, inability to penetrate cell membranes, and limited drug effectiveness. Ligand $\mathbf{D_4}$ (Fig. 22C) can penetrate cellular and nuclear membranes by conjugating **D1** to a polyamine derivative side chain.[243] In the DM1 cell model, $\mathbf{D_4}$ disperses $(CUG)_{960}$ ribonuclear foci (a hallmark of DM1 cells from MBNL1-CUG^{exp} aggregate) and releases MBNL1. Besides, $\mathbf{D_4}$ partially reverses the missplicing of insulin receptor pre-mRNA. Zimmerman *et al.*[244,245] designed a system for the analysis of MBNL1-CUG^{exp} inhibitors, ligands and MBNL1 formed complexes on $(CUG)_4$. The oligomylamine-linked ligand $\mathbf{D_9}$ (Fig. 22C) showed effective inhibition of the formation of the $(CUG)_{12}$·MBNL1 complex due to greater affinity to $(CUG)_6$.

Acridine-containing ligands $\mathbf{D_1}$–$\mathbf{D_5}$ and $\mathbf{D_9}$ (Fig. 22C) may undergo undesirable off-target activity and exhibit an unacceptably high level of inherently cytotoxicity, which limits their application *in vivo*. Zimmerman *et al.*[246] obtained $\mathbf{D_7}$ (Fig. 22C) by connecting two triaminotriazine units to target A-form RNA using the bisamidinium unit as the binding moiety. Ligand $\mathbf{D_1}$ can selectively bind to a single T–T/U–U mismatch, while $\mathbf{D_7}$ can target three consecutive CUG units. Ligand $\mathbf{D_7}$ has a very good affinity for $r(CUG)_{12}$ and can effectively destroy the interaction of MBNL1-$r(CUG)_{12}$. $\mathbf{D_7}$ can penetrate cell membranes and nuclei with negligible toxicity. In a DM1 Drosophila model, $\mathbf{D_7}$ dissolved MBNL1-$r(CUG)^{exp}$ ribonuclear foci, restored missplicting of insulin receptors and cardiac troponin T, and inhibited $r(CUG)^{exp}$ RNA-induced toxicity.

RNase catalyzes the degradation of RNA and cleaves the 3′ end of single-stranded unpaired C and U residues. A number of RNase A analog molecules have been designed.[247,248] Binding CUG^{exp} does not reverse all disease pathways, destroying toxic RNA transcripts or inhibiting their formation is an important to study.[249–251] Nguyen *et al.*[252] proposed ligands $\mathbf{D_5}$ and $\mathbf{D_6}$ (Fig. 22C) with side-chains at the 2- or 4-position of the acridine ring and $\mathbf{D_8}$ (Fig. 22C) with side-chains attached to the triaminotriazine rings aimed at multi-target treatment. *In vitro*, these ligands showed similar activity to RNase A to selectively cleave $(CUG)_{16}$. In a DM1 Drosophila model, they can inhibit CTG^{exp} transcription and sequestrate the nuclear foci of MBNL1.

Ligand drug $\mathbf{D_1}$ (Fig. 22A) is a simple triaminotriazine-acridine conjugate that recognizes T–T and U–U mismatches *via* hydrogen bonding (Fig. 22B).[253–256] The equilibrium dissociation constants

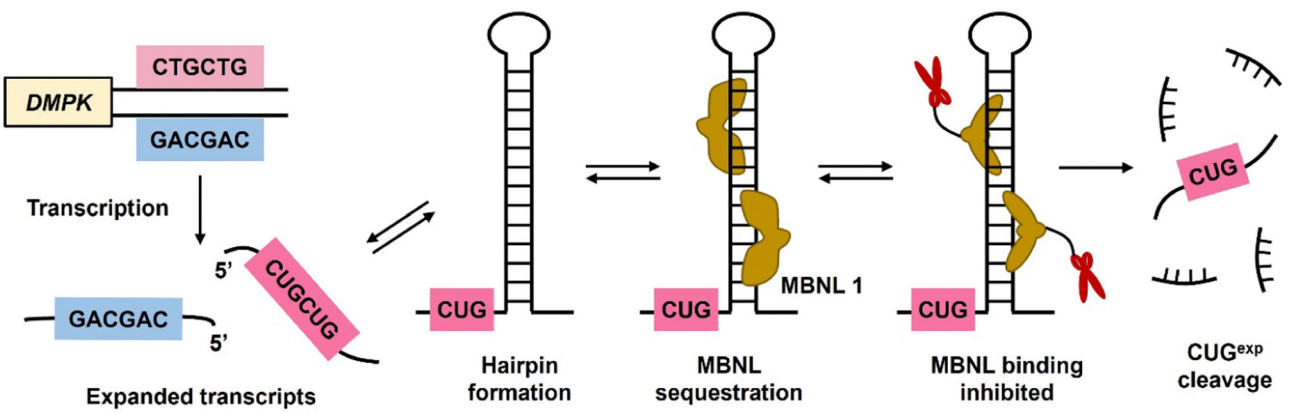

Fig. 21 CTG repeat expansion in *DMPK* gene produces expanded transcripts, CUG^{exp} sequesters splicing regulator MBNL1.[241] Reproduced under the terms of the CC–BY Creative Commons Attribution 3.0 Unported license (https://creativecommons.org/licenses/by/3.0).

 This journal is © The Royal Society of Chemistry 2024

Published on 03 January 2024. Downloaded by Yunnan University on 8/4/2025 1:35:41 AM.

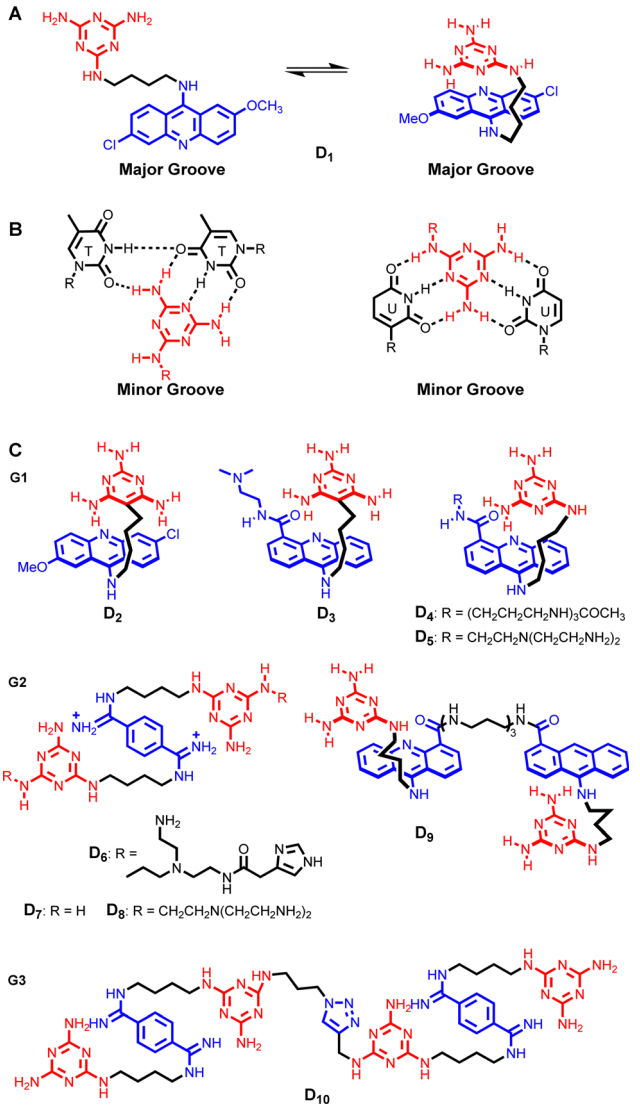

Fig. 22 (A) Chemical structure of ligand $\mathbf{D_1}$.[253] (B) Binding mode of $\mathbf{D_1}$ to T–T/U–U mismatch.[244–246] (C) The designed ligands of three generations G1, G2, and G3. $\mathbf{D_2}$–$\mathbf{D_3}$ aimed at DM2 and $\mathbf{D_4}$–$\mathbf{D_9}$ aimed at DM1.[247–257]

(K_d) of $\mathbf{D_1}$ for T–T and U–U pairs in d(CTG) and r(CUG) were 390 ± 80 nM and 430 ± 110 nM, respectively, which are much higher than that of C–C, A–A and G–G mismatches. $\mathbf{D_1}$ showed better affinity for T–T and U–U mismatch than C–C, A–A and G–G. Ligand $\mathbf{D_1}$ strongly and selectively binds CUG in RNA and inhibits binding of MBNL1.

The aforementioned ligands can be classified into two generations. The first-generation ligands $\mathbf{D_1}$–$\mathbf{D_5}$ hold only one triaminotriazine recognition unit, while the second-generation ligands $\mathbf{D_6}$–$\mathbf{D_9}$ have two. The third-generation ligand $\mathbf{D_{10}}$ (Fig. 22C), formed by linking two $\mathbf{D_7}$ units, is a potent inhibitor for MBNL1-rCUG^{exp}.[257] Compared to monomeric compound $\mathbf{D_7}$, $\mathbf{D_{10}}$ has a almost 1000-fold lower inhibition constant K_i (25 ± 8 nm) than $\mathbf{D_7}$ (189 ± 32 μm) for inhibition of MBNL1-$(CUG)_{16}$. The toxicity of benzamidinium-based $\mathbf{D_{10}}$ to HeLa cell was negligible at lower concentrations *versus* acridine-based dimeric ligands. 1 μM $\mathbf{D_{10}}$ was as active as 100 μM $\mathbf{D_7}$ in MBNL1-rCUG^{exp} nuclear foci dispersion, but no complete foci dispersion was observed at 100 μM. Meanwhile, $\mathbf{D_{10}}$ at lower concentration cannot fully correct the insulin receptor splicing defect than $\mathbf{D_7}$. In addition, the insufficient cellular penetration of $\mathbf{D_{10}}$ was due to its high molecular weight (M_r = 1166.4 Da) and the abundant hydrogen bonding donors and receptors.[258] In a DM1 Drosophila model, $\mathbf{D_{10}}$ improved two separate disease phenotypes, larval crawling defect and adult external eye degeneration.

The use of multivalency is an effective way to develop biological inhibitors.[259,260] Zimmerman *et al.*[261,262] developed multivalent ligands that bind to CTG^{exp} and CUG^{exp} using cell-penetrating peptide mimics, which reduced unwanted cytotoxicity and increased local drug concentrations, resulting in a multivalent effect that enhanced selectivity and affinity.[244,245,263] Zimmerman *et al.*[264] established a ligand screening method to identify dimers that bind to d(CTG)^{exp} and inhibit r(CUG)^{exp} and r(CAG)^{exp} production. This method is suitable for trinucleotide repeat diseases and targeting nucleic acid sequences associated with other diseases.

4.2 Molecular assembly for advanced drug delivery

Supramolecular polymers facilitate the dissolution, transport and controlled release of small molecule agents, bioactive proteins or other effective vectors relevant to therapy.[265,266] Drugs can be added to self-assembled peptides as cogroups through hydrolysis to promote sustained and local drug release on the basis of supramolecular hydrogels.[35,267,268] Aliphatic hybridized peptides encapsulate insoluble drugs within their hydrophobic nuclei and serve as effective drug carriers.[269] Supramolecular interactions can be used to regulate drug release kinetics.

The enzymes produced by cancer cells were used to induce control of supramolecular assembly. They can change the conformation of supramolecular nanostructures and promote the release of chemotherapeutic agents. Ulijn *et al.*[270] developed a peptide-based enzymatic reaction system capable of undergoing morphological changes from micelle aggregations to fibers *via* intramolecular hydrogen bonding during matrix metalloproteinases (MMPs)-9 cleavage. Through morphological changes, doxorubicin payload was retained in the formed fibers for slow release of anticancer drugs. The assembled fibers provide scaffold for local drug delivery due to the partial encapsulation of the drug and the biodegradable nature of the peptide carrier itself. The system also responds specifically to other MMPs and specifically to MMP-2 due to the overlap of specific spectra *in vivo*.

The structure of the anticancer drug methotrexate (MTX) is like that of melamine, can form complementary hydrogen bonds with cyanuric acid. Zhang *et al.*[271] synthesized a tumor-targeting amphiphilic peptide and conjugated cyanuric acid to the hydrophobic tail of the peptide (Fig. 23). In aqueous solution, the hydrophobic interactions between hydrophobic tails of amphiphilic peptides promoted the aggregation of molecules to form spherical micelles. The complementary hydrogen bonding interactions between terminal cyanate groups and MTX increased the hydrophobicity of the system,

Published on 03 January 2024. Downloaded by Yunnan University on 8/4/2025 1:35:41 AM.

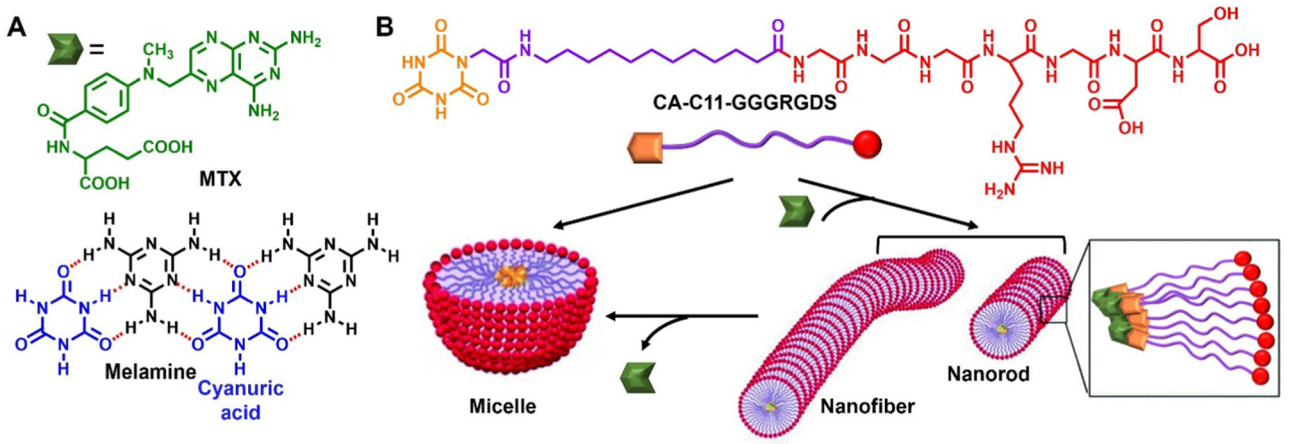

Fig. 23 (A) Molecular structures of methotrexate (MTX) and hydrogen bonding of cyanuric acid and melamine, and (B) assembly of amphiphilic peptide with MTX.[271]

resulting in the formation of MTX-loaded nanorods or nanofibers. MTX release disrupted the hydrophilic and hydrophobic balance, and micelles were recovered from the nanorods or nanofibers. The MTX-loaded nanorods targeted tumor cells with cytotoxicity (IC_{50} = 0.38 mg L^{-1}) more than twice that of normal cells.

The acidic environment of tumor sites and inflammatory tissues enables them to induce the release of antitumor and anti-inflammatory drugs. Hydrogen bonding rupture in acidic media leads to the decomposition of micellar aggregates for pH responsive drug delivery. Zhu *et al.*[272] prepared supramolecular nucleoside phospholipids with hydrogen bonding. Uridine functionalized phosphatidylcholine or phosphatidylethanolamine were used as hydrophilic head. And adenosine functionalized myristic acid and oleic acid were used as hydrophobic tails. Due to their amphiphilic properties, liposome-like bilayer nanovesicles were further self-assembled in aqueous solution. The acid responsiveness of hydrogen bonds enables the vesicles to disassemble in acidic environments. Supramolecular liposomes loaded with doxorubicin showed higher antitumor activity than traditional liposomes constructed from 1,2-dioleoyl-*sn*-glycero-3-phosphocholine. Zhu *et al.*[273] assembled two anticancer drugs purine nucleoside analogues chlorfarabine and folate analogues raltitrexed into clear structure nanoparticles with high quantitative drug loading through hydrogen bonding interactions. Clofarabine/raltitrexed nanoparticles improved the synergistic effect by blocking more cell cycle G1 phases and reducing the intracellular deoxynucleotide pools. Nanodrugs increased the blood retention half-life of free drugs, improved the drugs accumulation at tumor sites and promoted the synergistic antitumor performance *in vivo*.

Cao *et al.*[274] prepared HOF (PFC-1, surface area 2122 m^2 g^{-1}) with 1,3,6,8-tetrakis (*p*-benzoic acid) pyrene. Doxorubicin was encapsulated in Nano-PFC-1 and showed low cytotoxicity and excellent chemo-photodynamic effects in cancer therapy (HeLa cells). Sun *et al.*[275] prepared HOF (TCPP-1,3-DPP) using meso-tetra(carboxy-phenyl)-porphyrin (TCPP) with 1,3-di(4-pyridyl) propane (1,3-DPP). TCPP and DPP were connected by hydrogen bonds, carboxylic acid-pyridine supramolecular synthesizer, to form 1D porous stripes. The 1D stripes were stacked into 3D framework by π–π interactions. TCPP-1,3-DPP can slip outwards under pressure and the morphology of HOF changes from prismatic to 2D nanocrystal. Sun *et al.*[276] separated the 1D porous stripes from the TCPP-1,3-DPP structure using the ultrasound-assisted liquid stripping technology. Nanoribbons with atomic thickness (nr-HOF) have good dispersibility and large specific surface in aqueous solution. Porphyrins produced singlet oxygen under light in oxygen-containing environment, giving nr-HOF@Doxo the properties of photodynamic therapy. nr-HOF@Doxo was very effective and has a cell survival rate of 1.3%.

4.3 Indicator displacement strategy for DNA detection

Fluorescence biosensors based on nucleic acid is an important technology in the field of analytical chemistry and biochemistry.[277–279] Aggregation induced emission (AIE) is an unusual photo emission phenomenon, and its mechanism is the restriction of intramolecular rotations (RIR).[280] AIE molecules have been applied as fluorescent techniques for DNA detection through hydrogen bonding interactions within base pairing.[281] Controllable fluorescence supramolecular polymers with AIE properties can be prepared by modifying the molecular structure of AIE through multiple hydrogen bonding interactions. These supramolecular structures restrict the active intramolecular rotations of AIE molecule.[282]

Tang *et al.*[283] created a DNA probe TPE-T by decorating tetraphenylethene (TPE) with thymine motif (Fig. 24A). Adenine-rich ssDNA triggered fluorescence of AIE-containing TPE-T. The fluorescence was caused by RIM process induced by hydrogen bonds formation between thymine of the TPE-T molecules and adenine in ssDNA. TPE-T showed superb specificity for adenine containing ssDNA. Yang *et al.*[284] incorporated a base analog diaminopurine in TPE derivatives to extend the detection of ssDNA in water solutions. The obtained TPE-NH_2 (Fig. 24B) was proposed to link up ssDNA *via* electrostatic interactions or hydrogen bonding between the bases. In

 This journal is © The Royal Society of Chemistry 2024

Published on 03 January 2024. Downloaded by Yunnan University on 8/4/2025 1:35:41 AM.

detecting ssDNA, TPE units aggregated with DNA strands through hydrophobic interactions, resulting in enhanced fluorescence. The detection of poly deoxyadenylic acid with high selectivity in solution was carried out by forming chemical sensing ensemble with phenol red and TPE-NH_2. The strategy is to improve selectivity by reducing background fluorescence.

4.4 Bio-inspired adhesive hydrogels for tissue engineering

Cell-biomaterial interactions and biological environment are important in implantation biomaterials.[285] Supramolecular polymers are degradable and mechanically adjustable, providing a favourable biological environment to encapsulate bioactive ingredients growth factors and cells, stimulate the continuous growth of tissues.[265,286]

A peptidyl supramolecular polymer is a kind of bioactive material used in tissue engineering. Akashi *et al.*[287] constructed an injectable fibrous with a triple helix structure by hydrogen bonding using multi-arm PEG and collagen mimetic peptide. This hydrogel can be used as tissue crosslinking agent and drug carrier for cornea and can also be used for tissue engineering of skin, cartilage, and bone. Polydopamine (PDA) has strong adhesion to a variety of substrates and can promote cell attachment and proliferation. Lu *et al.*[288] prepared a hydrogel dressing PDA–CS–PAM for the treatment of cartilage regeneration without growth factors (Fig. 25). The non-covalent interaction between catechol-group-enriched polydopamine–chondroitin sulfate (PDA–CS) and covalent cross-linked polyacrylamide (PAM) network makes the hydrogel has super toughness and elasticity. PDA with adhesive catechol groups endowed the hydrogel with good cell affinity and high tissue adhesiveness. The CS and PDA components in the hydrogel create a suitable biomimetic extracellular matrix microenvironment to induce cartilage regeneration without the need for any chondrogenic cytokines. The hydrogel enhanced the adsorption and fixation of blood clots, and further induced tissue regeneration in the defect.

UPy-based supramolecular polymers synthesized through quadruple hydrogen bonding show low temperature processing performance, good degradation, and biocompatibility, which can be used for the preparation of bioactive polymer scaffolds.[289] Meijer *et al.*[290] prepared biomaterials using Upy-modified oligocaprolactone and Upy-functionalized UPy-Pro-His-Ser-Arg-Asn and UPy-Gly-Arg-Gly-Asp-Ser peptide sequences. The material showed good biodegradability, biocompatibility, and mechanical properties, and possessed specific binding ability with fibroblast to promote cell proliferation. The end group functionalized UPy-oligocaprolactone ($PCL_{2000}UPy_2$) and the chain extended UPy-oligocaprolactone ($PCL_{1250}UPy_6$) were formed through quadruple hydrogen bonding interactions.[291] The blend obtained by mixing the two polymers (2 : 8) showed good mechanical properties, very mild foreign body reaction and no deformation or crystallization after implanted into male Albino Oxford rats. The performance of scaffold materials can be tuneed according to requirements using the bioactive factors synthesized by self-complementary hydrogen bonding units UPy. Guo *et al.*[292] synthesized a physical dual network hydrogel using catechol–Fe^{3+} coordination crosslinked poly(glycerol sebacate)-*co*-poly(ethylene glycol)-*g*-catechol and quadruple hydrogen bonding crosslinked UPy modified gelatin. The hydrogel can be used as wound dressing due to it has high hemostatic effect, accelerates wound healing, and has a higher killing rate against methicillin-resistant *Staphylococcus aureus.*

4.5 Self-assembly complexes as gene delivery vectors for gene transfection

With the progress of medical technology, gene therapy has become a common method to treat gene diseases, such as cancer and autoimmune/mutation-induced metabolic syndromes. Traditional non-viral vectors used in gene therapy, such as cationic phospholipids, polypeptides, and polymers, can efficiently compress DNA to achieve good gene transfection, but they have disadvantages such as complex preparation methods and lack of responsiveness. Supramolecular polymers constructed by small molecule building units through non-covalent interactions possess controllable structures and can be depolymerized when stimulated by external stimuli. Supramolecular polymers produce incomparable advantages when applied in gene therapy.

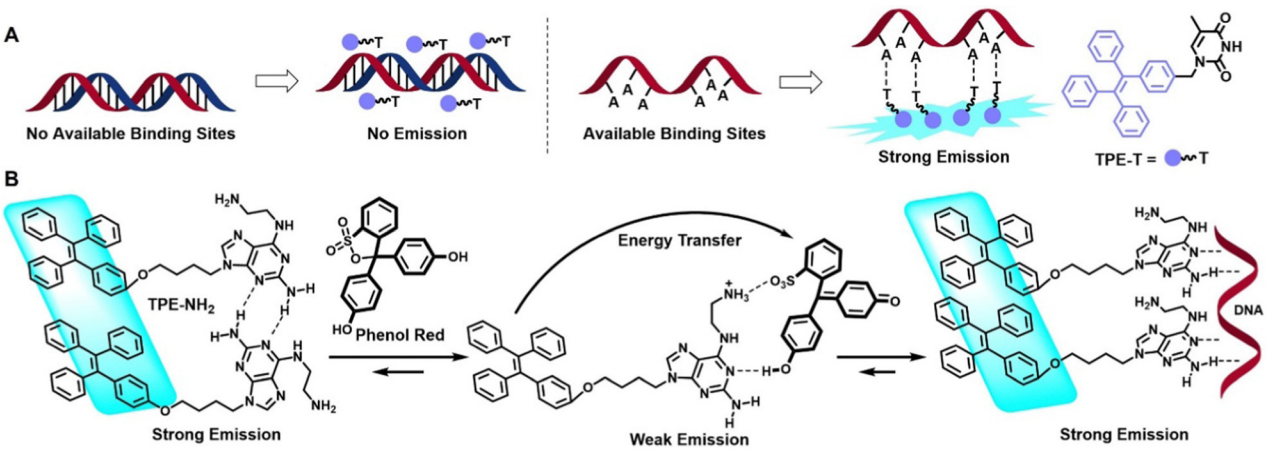

Fig. 24 (A) ssDNA detection by TPE-T through hydrogen bonding between base pairs (T–A).[283] (B) DNA detection by TPE-NH_2 using indicator-displacement strategy, phenol red formed chemo-sensing ensemble with TPE-NH_2.[284]

Published on 03 January 2024. Downloaded by Yunnan University on 8/4/2025 1:35:41 AM.

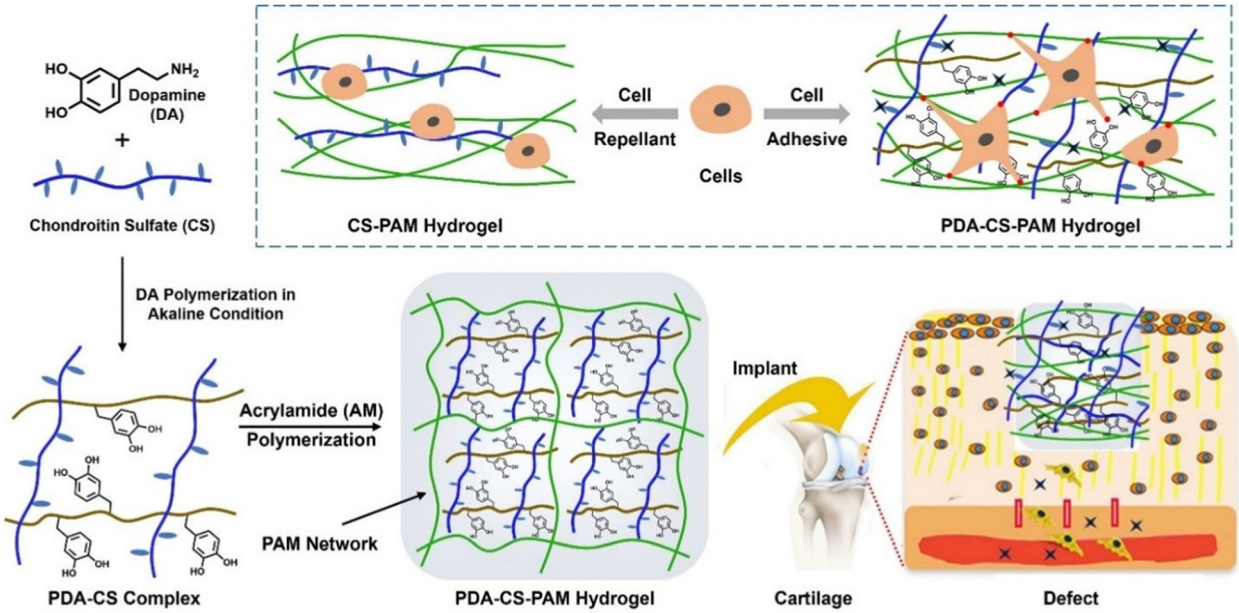

Fig. 25 The tissue-adhesive hydrogels PDA–CS–PAM for cartilage regeneration.[288]

Liu *et al.*[293] prepared hydrogen bonding strengthened hydrogel using 2-vinyl-4,6-diamino-1,3,5-triazine (VDT) and poly(ethylene glycol) methacrylated β-cyclodextrin (PEG-β-CD). The bases of plasmid DNA are anchored to the hydrogel by hydrogen bonding with diaminotriazine, allowing for reverse gene transfection of luciferase gene in African green monkey kidney cells cultured on the gel surface. PEG-β-CD can encapsulate hydrophobic drugs, and the smaller the amount of its copolymerization, the higher the release rate of ibuprofen. Gao *et al.*[294] synthesized quaternary complex pDNA-TPE/BSA (PDTB) for intracellular imaging and gene transfection through non-covalent interactions (hydrophobic, hydrogen bonding, electrostatic interactions, *etc.*) (Fig. 26). Gene transfection was achieved due to bovine serum albumin (BSA) promoted dissociation of the polymer after protonation, tetraphenylethylene derivatives (TPE) reduced endosomal membrane stability and enhanced endosomal escape of pDNA payload. The positive surface charge of PDTB was lower than that of PD, and the addition of biocompatible BSA was helpful to improve cell viability. The AIE property of TPE enabled the polymer to stably track the delivery of pDNA into cancer cells.

Cheng *et al.*[295] developed gene vectors with low-generation dendrimers. DAT was modified on the generation 3 (G3) polyamide (PAMAM) dendrimer with an average of 13 DAT moieties per G3 dendrimer, forming G3-DAT_{13}. Cyanuric acid (CyA) formed supramolecular complex with G3-DAT_{13}/DNA, which effectively delivered genes through hydrogen bond recognition. Without CyA, the transfection efficacy of EGFP with G3-DAT_{13} on HEK293 cells was less than 1%. While in the presence of CyA, EGFP expression efficacy was more than 20%. CyA can increase cellular uptake of the G3-DAT_{13}/DNA complex without

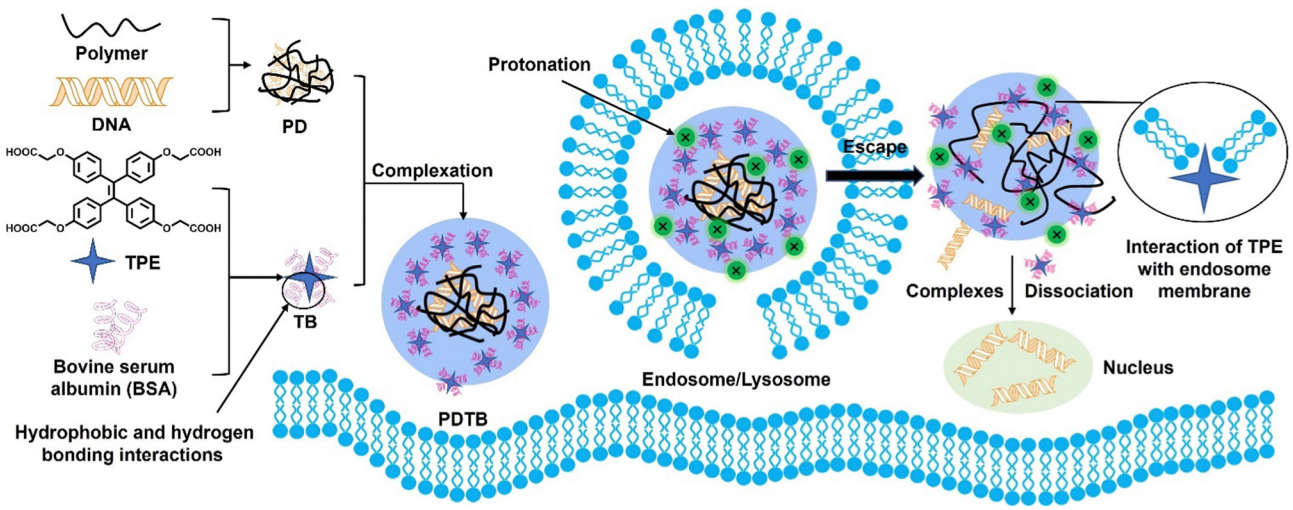

Fig. 26 Schematic representation of PDTB complexes as gene delivery vectors.[294]

 This journal is © The Royal Society of Chemistry 2024

Published on 03 January 2024. Downloaded by Yunnan University on 8/4/2025 1:35:41 AM.

introducing additional toxicity to transfected cells. This supramolecular approach provides an innovative concept for designing non-viral gene delivery vectors. In addition, Cheng *et al.*[296] used hydrogen bonding and hydrophobic interactions of natural polyphenol (−)-epigallocatechin-3-*O*-gallate (EGCG) to bind siRNA to form nanoparticles which were negatively charged, helping low molecular weight cationic polymers bind siRNA to uniform size green nanoparticles (GNPs) at low doses. Compared with low molecular weight cationic polymers alone, GNPs significantly improved siRNA delivery efficiency and effectively silenced multiple target genes in a variety of cells. Because EGCG is a pure natural green plant extract, the low molecular weight cationic polymer has low cytotoxicity, and the complex shows excellent biocompatibility. *In vivo* experiments, GNPs inhibited TNF-α expression by effectively silencing PHD2 gene. It effectively reduced chronic intestinal inflammation in inflammatory bowel disease model. This supramolecular method can be used in low molecular weight cationic polymers with different molecular weight, chemical composition, and topological structure. It is a universal, high efficiency, and low toxicity method for siRNA delivery.

5. Conclusions and perspectives

Supramolecular polymers possess dynamically switchable structures and peculiar functions compared to traditional polymers, which are endowed with reversible non-covalent interactions. A single hydrogen bond is not strong enough to form stable self-assembled structures. Fortunately, multiple hydrogen bonding modules are desirable nano-adhesion promoters and ideal building blocks for the reasonable design of polymer blends, IPNs, and energy dissipation materials due to their exceptional specificity, binding affinity, and stimulus response. Tautomerism, self-recognition and competing equilibria of hydrogen bonding motifs, temperature, and types of solvents all influence the structure of supramolecular polymers. The controllable synthesis of hydrogen bonding supramolecular polymers with the assembly process is achieved by many methods, for example, covalent polymerization of supramolecular functional monomers, *in situ* self-sorting process, combination with interfacial polymerization, kinetically controlled living supramolecular polymerization, orthogonal non-covalent interactions. There is growing interest in multiple hydrogen bonding recognition systems for supramolecular architectures, chiral supramolecular assemblies, stimuli responsive polymers, IPNs, HOFs, adhesive supramolecules, and energy dissipater. The quantitative analysis of hydrogen bonding interactions is fundamental yet significant for designing advanced material. The single pair rupture forces of multiple hydrogen bonding modules can be measured by AFM and SMFS. The studies reviewed here demonstrate the potential of multiple hydrogen bonding stimulated supramolecular architectures in biomedical application, including drug design, drug delivery, bio-detection, tissue engineering, and gene transfection, and showcase the role of nature as a source of inspiration.

From the practical application perspective, many meaningful supramolecular building units and systems are still at the monomer design stage. Available versatile hydrogen bonding systems are still quite limited for constructing specific supramolecular materials. Noteworthy, supramolecular systems in organisms are almost dynamic with continuous recognition, production, consumption, and transmission, which are superior compared to the relatively static supramolecular self-assembly approach. These basic challenges remain to be solved before much broader practical applications. Multiple hydrogen bonding alone is not enough for obtaining multidimensional and multifunctional supramolecular polymers, only if other non-covalent interactions are fused together. It is foreseen that more innovative supramolecular functional materials will emerge and play an important role in expanded practical fields, not limited to the examples highlighted in this review.

Author contributions

Yanxia Liu: investigation, methodology, data curation, visualization, writing – original draft preparation, writing – review and editing. Lulu Wang: investigation, methodology, software, formal analysis, writing – original draft preparation. Lin Zhao: investigation, methodology, data curation, visualization. Yagang Zhang: conceptualization, formal analysis, methodology, supervision, writing – original draft preparation, writing – review and editing, resources, project administration, funding acquisition. Zhanting Li: conceptualization, formal analysis, methodology, supervision, writing – review and editing. Feihe Huang: conceptualization, formal analysis, methodology, supervision, writing – review and editing.

Conflicts of interest

The authors declare no conflict of interest.

Acknowledgements

Y. Zhang acknowledges the financial support from Key Research and Development Projects of Sichuan Province (2023YFG0222), the Tianfu Emei Science and Technology Innovation Leader Program in Sichuan Province (2021), the University of Electronic Science and Technology of China Talent Start-up Funds (A1098 5310 2360 1208) and the National Natural Science Foundation of China (21472235, 21464015). The authors thank Prof. Chuanbing Tang and Prof. Steven C. Zimmerman for helpful discussion and valuable advice and suggestions.

References

1 H. Peng, W. Zhu, W. J. Guo, Q. Li, S. Ma, C. Bucher, B. Liu, X. Ji, F. Huang and J. L. Sessler, *Prog. Polym. Sci.*, 2023, **137**, 101635.
2 G. T. Williams, C. J. E. Haynes, M. Fares, C. Caltagirone, J. R. Hiscock and P. A. Gale, *Chem. Soc. Rev.*, 2021, **50**, 2737–2763.

Published on 03 January 2024. Downloaded by Yunnan University on 8/4/2025 1:35:41 AM.

3 J. M. Lehn, *Chem. Soc. Rev.*, 2017, **46**, 2378–2379.
4 Y. Zhu, W. Zheng, W. Wang and H. Yang, *Chem. Soc. Rev.*, 2021, **50**, 7395–7417.
5 W. Eli and Y. Zhang, *Curr. Org. Chem.*, 2013, **17**, 3064–3072.
6 F. Robert, *Science*, 2005, **309**, 95.
7 L. Fang, M. A. Olson, D. Benítez, E. Tkatchouk, W. A. Goddard III and J. F. Stoddart, *Chem. Soc. Rev.*, 2010, **39**, 17–29.
8 S. Han, S. Pensec, D. Yilmaz, C. Lorthioir, J. Jestin, J.-M. Guigner, F. Niepceron, J. Rieger, F. Stoffelbach, E. Nicol, O. Colombani and L. Bouteiller, *Nat. Commun.*, 2020, **11**, 4760.
9 T. Steiner, *Angew. Chem., Int. Ed.*, 2002, **41**, 48–76.
10 G. Thangavel, M. W. M. Tan and P. S. Lee, *Nano Convergence*, 2019, **6**, 29.
11 T. Xiao, L. Zhou, X. Q. Sun, F. Huang, C. Lin and L. Wang, *Chin. Chem. Lett.*, 2020, **31**, 1–9.
12 L. J. Karas, C.-H. Wu, R. Das and J. I.-C. Wu, *Wiley Interdiscip. Rev.: Comput. Mol. Sci.*, 2020, **10**, e1477.
13 Y. F. Huo, Z. F. He, C. Wang, L. Zhang, Q. Y. Xuan, S. Y. Wei, Y. H. Wang, D. Pan, B. B. Dong, R. B. Wei, N. Naik and Z. H. Guo, *Chem. Commun.*, 2021, **57**, 1413–1429.
14 R. P. Sijbesma and E. Meijer, *Chem. Commun.*, 2003, 5–16.
15 F. H. Beijer, R. P. Sijbesma, H. Kooijman, A. L. Spek and E. Meijer, *J. Am. Chem. Soc.*, 1998, **120**, 6761–6769.
16 X. Ji, M. Ahmed, L. Long, N. M. Khashab, F. Huang and J. L. Sessler, *Chem. Soc. Rev.*, 2019, **48**, 2682–2697.
17 E. A. Dubiel, Y. Martin and P. Vermette, *Chem. Rev.*, 2011, **111**, 2900–2936.
18 C. Rodriguez-Emmenegger, S. Janel, A. de los Santos Pereira, M. Bruns and F. Lafont, *Polym. Chem.*, 2015, **6**, 5740–5751.
19 C. Heinzmann, C. Weder and L. M. de Espinosa, *Chem. Soc. Rev.*, 2016, **45**, 342–358.
20 H. J. Busscher and H. C. van der Mei, *PLoS Pathog.*, 2012, **8**, e1002440.
21 Q. Zhang, T. Li, A. Duan, S. Dong, W. Zhao and P. J. Stang, *J. Am. Chem. Soc.*, 2019, **141**, 8058–8063.
22 K. Yamauchi, J. R. Lizotte and T. E. Long, *Macromolecules*, 2003, **36**, 1083–1088.
23 P. Cordier, F. Tournilhac, C. Soulié-Ziakovic and L. Leibler, *Nature*, 2008, **451**, 977–980.
24 L. Song, T. Zhu, L. Yuan, J. Zhou, Y. Zhang, Z. Wang and C. Tang, *Nat. Commun.*, 2019, **10**, 1315.
25 J. Wu, H. Lei, J. Li, Z. Zhang, G. Zhu, G. Yang, Z. Wang and Z. Hua, *Chem. Eng. J.*, 2021, **405**, 126976.
26 A. C. Ferahian, D. K. Hohl, C. Weder and L. Montero de Espinosa, *Macromol. Mater. Eng.*, 2019, **304**, 1900161.
27 M. S. Ganewatta, Z. Wang and C. Tang, *Nat. Rev. Chem.*, 2021, **5**, 753–772.
28 J. M. Lehn, *Chem. Soc. Rev.*, 2007, **36**, 151–160.
29 S. G. Chen, Y. Yu, X. Zhao, Y. Ma, X. K. Jiang and Z. T. Li, *J. Am. Chem. Soc.*, 2011, **133**, 11124–11127.
30 J. Luo, T. Lei, L. Wang, Y. G. Ma, Y. Cao, J. Wang and J. Pei, *J. Am. Chem. Soc.*, 2009, **131**, 2076–2077.
31 F. Gao, Y. C. Tan, Y. Yu, H. Chen and Y. G. Ma, *Supramol. Chem.*, 2011, **23**, 753–758.
32 L. S. Shimizu, *Polym. Int.*, 2007, **56**, 444–452.
33 D. C. Sherrington and K. A. Taskinen, *Chem. Soc. Rev.*, 2001, **30**, 83–93.
34 Y. Liu, Z. Wang and X. Zhang, *Chem. Soc. Rev.*, 2012, **41**, 5922–5932.
35 S. Bernhard and M. W. Tibbitt, *Adv. Drug Delivery Rev.*, 2021, **171**, 240–256.
36 M. Wehner and F. Würthner, *Nat. Rev. Chem.*, 2020, **4**, 38–53.
37 L. Voorhaar and R. Hoogenboom, *Chem. Soc. Rev.*, 2016, **45**, 4013–4031.
38 R. B. Lin, Y. He, P. Li, H. Wang, W. Zhou and B. Chen, *Chem. Soc. Rev.*, 2019, **48**, 1362–1389.
39 Z. L. Xie, B. L. Hu, R. W. Li and Q. C. Zhang, *ACS Omega*, 2021, **6**, 9319–9333.
40 P. K. Hashim, J. Bergueiro, E. W. Meijer and T. Aida, *Prog. Polym. Sci.*, 2020, **105**, 101250.
41 P. Song and H. Wang, *Adv. Mater.*, 2020, **32**, 1901244.
42 L. Y. Zhao, Y. M. Liu, R. R. Xing and X. H. Yan, *Angew. Chem.*, 2020, **59**, 3793–3801.
43 L. Saunders and P. X. Ma, *Macromol. Biosci.*, 2019, **19**, 1800313.
44 D. B. Amabilino, D. K. Smith and J. W. Steed, *Chem. Soc. Rev.*, 2017, **46**, 2404–2420.
45 X. Du, J. Zhou, J. Shi and B. Xu, *Chem. Rev.*, 2015, **115**, 13165–13307.
46 G. Armstrong and M. Buggy, *J. Mater. Sci. Technol.*, 2005, **40**, 547–559.
47 E. L. Florin, V. T. Moy and H. E. Gaub, *Science*, 1994, **264**, 415–417.
48 Y. Kyogoku, R. Lord and A. Rich, *Biochim. Biophys. Acta, Nucleic Acids Protein Synth.*, 1969, **179**, 10–17.
49 Y. Kyogoku, R. Lord and A. Rich, *Proc. Natl. Acad. Sci. U. S. A.*, 1967, **57**, 250–257.
50 J. H. G. Steinke, I. R. Dunkin and D. C. Sherrington, *Trends Anal. Chem.*, 1999, **18**, 159–164.
51 T. J. Murray and S. C. Zimmerman, *J. Am. Chem. Soc.*, 1992, **114**, 4010–4011.
52 J. Pranata, S. G. Wierschke and W. L. Jorgensen, *J. Am. Chem. Soc.*, 1991, **113**, 2810–2819.
53 W. L. Jorgensen and J. Pranata, *J. Am. Chem. Soc.*, 1990, **112**, 2008–2010.
54 P. S. Corbin and S. C. Zimmerman, *J. Am. Chem. Soc.*, 1998, **120**, 9710–9711.
55 D. A. Bell and E. V. Anslyn, *Tetrahedron*, 1995, **51**, 7161–7172.
56 S. Djurdjevic, D. A. Leigh, H. McNab, S. Parsons, G. Teobaldi and F. Zerbetto, *J. Am. Chem. Soc.*, 2007, **129**, 476–477.
57 B. A. Blight, A. Camara-Campos, S. Djurdjevic, M. Kaller, D. A. Leigh, F. M. McMillan, H. McNab and A. M. Slawin, *J. Am. Chem. Soc.*, 2009, **131**, 14116–14122.
58 M. Papmeyer, C. A. Vuilleumier, G. M. Pavan, K. O. Zhurov and K. Severin, *Angew. Chem.*, 2016, **55**, 1685–1689.

 This journal is © The Royal Society of Chemistry 2024

Published on 03 January 2024. Downloaded by Yunnan University on 8/4/2025 1:35:41 AM.

59 A. J. Wilson, *Soft Matter*, 2007, **3**, 409–425.
60 P. Y. Dankers and E. Meijer, *Bull. Chem. Soc. Jpn.*, 2007, **80**, 2047–2073.
61 T. F. de Greef and E. Meijer, *Nature*, 2008, **453**, 171.
62 T. F. de Greef, M. M. Smulders, M. Wolffs, A. P. Schenning, R. P. Sijbesma and E. Meijer, *Chem. Rev.*, 2009, **109**, 5687–5754.
63 C. C. Lee, C. Grenier, E. Meijer and A. P. Schenning, *Chem. Soc. Rev.*, 2009, **38**, 671–683.
64 C. Schmuck and W. Wienand, *Angew. Chem., Int. Ed.*, 2001, **40**, 4363–4369.
65 J. D. Fox and S. J. Rowan, *Macromolecules*, 2009, **42**, 6823–6835.
66 R. P. Sijbesma, F. H. Beijer, L. Brunsveld, B. J. Folmer, J. K. Hirschberg, R. F. Lange, J. K. Lowe and E. Meijer, *Science*, 1997, **278**, 1601–1604.
67 B. J. Folmer, R. Sijbesma, R. Versteegen, J. Van der Rijt and E. Meijer, *Adv. Mater.*, 2000, **12**, 874–878.
68 T. Park, M. F. Mayer, S. Nakashima and S. C. Zimmerman, *Synlett*, 2005, 1435–1436.
69 E. M. Todd and S. C. Zimmerman, *J. Am. Chem. Soc.*, 2007, **129**, 14534–14535.
70 T. Park and S. C. Zimmerman, *J. Am. Chem. Soc.*, 2006, **128**, 13986–13987.
71 T. Park and S. C. Zimmerman, *J. Am. Chem. Soc.*, 2006, **128**, 14236–14237.
72 T. Park and S. C. Zimmerman, *J. Am. Chem. Soc.*, 2006, **128**, 11582–11590.
73 C. A. Anderson, P. G. Taylor, M. A. Zeller and S. C. Zimmerman, *J. Org. Chem.*, 2010, **75**, 4848–4851.
74 P. S. Corbin, L. J. Lawless, Z. Li, Y. Ma, M. J. Witmer and S. C. Zimmerman, *Proc. Natl. Acad. Sci. U. S. A.*, 2002, **99**, 5099–5104.
75 G. Ligthart, H. Ohkawa, R. P. Sijbesma and E. W. Meijer, *J. Am. Chem. Soc.*, 2005, **127**, 810–811.
76 D. W. Kuykendall, C. A. Anderson and S. C. Zimmerman, *Org. Lett.*, 2008, **11**, 61–64.
77 T. Park, E. M. Todd, S. Nakashima and S. C. Zimmerman, *J. Am. Chem. Soc.*, 2005, **127**, 18133–18142.
78 Y. Hisamatsu, N. Shirai, S.-I. Ikeda and K. Odashima, *Org. Lett.*, 2010, **12**, 1776–1779.
79 Y. Hisamatsu, N. Shirai, S.-I. Ikeda and K. Odashima, *Org. Lett.*, 2009, **11**, 4342–4345.
80 X. Li, Y. Jia, Y. Ren, Y. Wang, J. Hu, T. Ma, W. Feng and L. Yuan, *Org. Biomol. Chem.*, 2013, **11**, 6975–6983.
81 S. K. Chang and A. D. Hamilton, *J. Am. Chem. Soc.*, 1988, **110**, 1318–1319.
82 H. Zeng, R. S. Miller, R. A. Flowers and B. Gong, *J. Am. Chem. Soc.*, 2000, **122**, 2635–2644.
83 M. Li, K. Yamato, J. S. Ferguson and B. Gong, *J. Am. Chem. Soc.*, 2006, **128**, 12628–12629.
84 A. Gooch, S. Barrett, J. Fisher, C. I. Lindsay and A. J. Wilson, *Org. Biomol. Chem.*, 2011, **9**, 5938–5940.
85 C. Schmuck and W. Wienand, *J. Am. Chem. Soc.*, 2003, **125**, 452–459.
86 M. F. Mayer, S. Nakashima and S. C. Zimmerman, *Org. Lett.*, 2005, **7**, 3005–3008.
87 W. J. Chu, Y. Yang and C.-F. Chen, *Org. Lett.*, 2010, **12**, 3156–3159.
88 J. Zhu, J. B. Lin, Y. X. Xu, X. B. Shao, X. K. Jiang and Z.-T. Li, *J. Am. Chem. Soc.*, 2006, **128**, 12307–12313.
89 J. Hu, J. Lu, R. Li and Y. Ju, *Soft Matter*, 2011, **7**, 891–894.
90 W. Yang, A. Greenaway, X. Lin, R. Matsuda, A. J. Blake, C. Wilson, W. Lewis, P. Hubberstey, S. Kitagawa and N. R. Champness, *J. Am. Chem. Soc.*, 2010, **132**, 14457–14469.
91 S. Chen, Z. Li, Y. Wu, N. Mahmood, F. Lortie, J. Bernard, W. H. Binder and J. Zhu, *Angew. Chem., Int. Ed.*, 2022, **61**, e202203876.
92 M. Wu, L. Yuan, F. Jiang, Y. Zhang, Y. He, Y. Z. You, C. Tang and Z. Wang, *Chem. Mater.*, 2020, **32**, 8325–8332.
93 B. L. Tardy, J. J. Richardson, L. G. Greca, J. Guo, H. Ejima and O. J. Rojas, *Adv. Mater.*, 2020, **32**, 1906886.
94 S. J. D. Lugger, S. J. A. Houben, Y. Foelen, M. G. Debije, A. P. H. J. Schenning and D. J. Mulder, *Chem. Rev.*, 2022, **122**, 4946–4975.
95 S. C. Zimmerman, F. Zeng, D. E. Reichert and S. V. Kolotuchin, *Science*, 1996, **271**, 1095–1098.
96 J. M. Lehn, *Pure Appl. Chem.*, 1994, **66**, 1961–1966.
97 P. S. Corbin and S. C. Zimmerman, *J. Am. Chem. Soc.*, 2000, **122**, 3779–3780.
98 P. S. Corbin, S. C. Zimmerman, P. A. Thiessen, N. A. Hawryluk and T. J. Murray, *J. Am. Chem. Soc.*, 2001, **123**, 10475–10488.
99 C. Zhou, X. Li, Z. Gong, C. Jia, Y. Lin, C. Gu, G. He, Y. Zhong, J. Yang and X. Guo, *Nat. Commun.*, 2018, **9**, 807.
100 P. A. Korevaar, S. J. George, A. J. Markvoort, M. M. Smulders, P. A. Hilbers, A. P. Schenning, T. F. De Greef and E. Meijer, *Nature*, 2012, **481**, 492–496.
101 Y. Nakano, A. J. Markvoort, S. Cantekin, I. A. W. Filot, H. M. M. ten Eikelder, E. W. Meijer and A. R. A. Palmans, *J. Am. Chem. Soc.*, 2013, **135**, 16497–16506.
102 M. Garzoni, M. B. Baker, C. M. Leenders, I. K. Voets, L. Albertazzi, A. R. Palmans, E. Meijer and G. M. Pavan, *J. Am. Chem. Soc.*, 2016, **138**, 13985–13995.
103 M. F. J. Mabesoone, A. R. A. Palmans and E. W. Meijer, *J. Am. Chem. Soc.*, 2020, **142**, 19781–19798.
104 K. Aratsu, R. Takeya, B. R. Pauw, M. J. Hollamby, Y. Kitamoto, N. Shimizu, H. Takagi, R. Haruki, S.-I. Adachi and S. Yagai, *Nat. Commun.*, 2020, **11**, 1623.
105 M. A. Gillissen, M. M. Koenigs, J. J. Spiering, J. A. Vekemans, A. R. Palmans, I. K. Voets and E. Meijer, *J. Am. Chem. Soc.*, 2013, **136**, 336–343.
106 S. Kheria, S. Rayavarapu, A. S. Kotmale and G. J. Sanjayan, *Chem. Commun.*, 2017, **53**, 2689–2692.
107 R. Wechsel, M. Žabka, J. W. Ward and J. Clayden, *J. Am. Chem. Soc.*, 2018, **140**, 3528–3531.
108 E. Mattia and S. Otto, *Nat. Nanotechnol.*, 2015, **10**, 111–119.
109 D. van der Zwaag, P. A. Pieters, P. A. Korevaar, A. J. Markvoort, A. J. H. Spiering, T. F. A. de Greef and E. W. Meijer, *J. Am. Chem. Soc.*, 2015, **137**, 12677–12688.
110 L. Yang, X. Tan, Z. Wang and X. Zhang, *Chem. Rev.*, 2015, **115**, 7196–7239.
111 S. Ogi, K. Sugiyasu, S. Manna, S. Samitsu and M. Takeuchi, *Nat. Chem.*, 2014, **6**, 188–195.

Published on 03 January 2024. Downloaded by Yunnan University on 8/4/2025 1:35:41 AM.

112 Q. Song, J. F. Xu and X. Zhang, *J. Polym. Sci., Part A: Polym. Chem.*, 2017, **55**, 604–609.
113 J. F. Xu, Y. Z. Chen, D. Wu, L. Z. Wu, C. H. Tung and Q. Z. Yang, *Angew. Chem., Int. Ed.*, 2013, **52**, 9738–9742.
114 L. Yang, X. Liu, X. Tan, H. Yang, Z. Wang and X. Zhang, *Polym. Chem.*, 2014, **5**, 323–326.
115 X. Liu, B. Qin, J.-F. Xu, Z. Wang and X. Zhang, *J. Photochem. Photobiol., A*, 2018, **355**, 414–418.
116 C. Talotta, C. Gaeta, Z. Qi, C. A. Schalley and P. Neri, *Angew. Chem., Int. Ed.*, 2013, **52**, 7437–7441.
117 X. Cheng, T. Miao, Y. Qian, Z. Zhang, W. Zhang and X. Zhu, *Int. J. Mol. Sci.*, 2020, **21**, 6186.
118 Z. Huang, L. Yang, Y. Liu, Z. Wang, O. A. Scherman and X. Zhang, *Angew. Chem., Int. Ed.*, 2014, **53**, 5351–5355.
119 Z. Huang, B. Qin, L. Chen, J.-F. Xu, C. F. J. Faul and X. Zhang, *Macromol. Rapid Commun.*, 2017, **38**, 1700312.
120 Y. Li, T. Park, J. K. Quansah and S. C. Zimmerman, *J. Am. Chem. Soc.*, 2011, **133**, 17118–17121.
121 B. Qin, S. Zhang, Q. Song, Z. Huang, J. F. Xu and X. Zhang, *Angew. Chem.*, 2017, **129**, 7747–7751.
122 A. Sarkar, R. Sasmal, A. Das, A. Venugopal, S. S. Agasti and S. J. George, *Angew. Chem., Int. Ed.*, 2021, **60**, 18209–18216.
123 S. Sarkar, A. Sarkar and S. J. George, *Angew. Chem., Int. Ed.*, 2020, **59**, 19841–19845.
124 L. J. Prins, D. N. Reinhoudt and P. Timmerman, *Angew. Chem., Int. Ed.*, 2001, **40**, 2382–2426.
125 M. Fujita, K. Umemoto, M. Yoshizawa, N. Fujita, T. Kusukawa and K. Biradha, *Chem. Commun.*, 2001, 509–518.
126 T. R. Kelly, C. Zhao and G. J. Bridger, *J. Am. Chem. Soc.*, 1989, **111**, 3744–3745.
127 M. Li, K. Yamato, J. S. Ferguson, K. K. Singarapu, T. Szyperski and B. Gong, *J. Am. Chem. Soc.*, 2008, **130**, 491–500.
128 S. Merget, L. Catti, S. Zev, D. T. Major, N. Trapp and K. Tiefenbacher, *Chem. – Eur. J.*, 2021, **27**, 4447.
129 L. Wang, G. T. Wang, X. Zhao, X. K. Jiang and Z. T. Li, *J. Org. Chem.*, 2011, **76**, 3531–3535.
130 M. J. Hardie, *Chem. Soc. Rev.*, 2010, **39**, 516–527.
131 H. Matsubara, A. Hasegawa, K. Shiwaku, K. Asano, M. Uno, S. Takahashi and K. Yamamoto, *Chem. Lett.*, 1998, 923–924.
132 I. Lijanova, J. Flores Maturano, J. Dominguez Chavez, K. Sánchez Montes, S. Hernandez Ortega, T. Klimova and M. Martínez-García, *Supramol. Chem.*, 2009, **21**, 24–34.
133 A. M. Koskinen, *Int. J. Biochem.*, 1994, **26**, 602.
134 P. Qin, Z. Wu, P. Li, D. Niu, M. Liu and M. Yin, *ACS Appl. Mater. Interfaces*, 2021, **13**, 18047–18055.
135 L. Zhang, H. Wang, S. Lia and M. Liu, *Chem. Soc. Rev.*, 2020, **49**, 9095–9120.
136 L. J. Prins, J. Huskens, F. de Jong, P. Timmerman and D. N. Reinhoudt, *Nature*, 1999, **398**, 498–502.
137 Y. Dorca, E. E. Greciano, J. S. Valera, R. Gómez and L. Sánchez, *Chem. – Eur. J.*, 2019, **25**, 5848–5864.
138 G. Markiewicz, M. M. J. Smulders and A. R. Stefankiewicz, *Adv. Sci.*, 2019, **6**, 1900577.
139 K. Salikolimi, V. K. Praveen, A. A. Sudhakar, K. Yamada, N. N. Horimoto and Y. Ishida, *Nat. Commun.*, 2020, **11**, 2311.
140 Q. Zhang, S. Crespi, R. Toyoda, R. Costil, W. R. Browne, D. H. Qu, H. Tian and B. L. Feringa, *J. Am. Chem. Soc.*, 2022, **144**, 4376–4382.
141 J. Liang, H. Zhang, A. Hao and P. Xing, *ACS Appl. Mater. Interfaces*, 2021, **13**, 29170–29178.
142 N. Veling, R. van Hameren, A. M. van Buul, A. E. Rowan, R. J. M. Nolte and J. A. A. W. Elemans, *Chem. Commun.*, 2012, **48**, 4371–4373.
143 J. A. Berrocal, M. F. J. Mabesoone, M. García Iglesias, A. Huizinga, E. W. Meijer and A. R. A. Palmans, *Chem. Commun.*, 2019, **55**, 14906–14909.
144 M. M. Green, M. P. Reidy, R. D. Johnson, G. Darling, D. J. O'Leary and G. Willson, *J. Am. Chem. Soc.*, 1989, **111**, 6452–6454.
145 L. J. Prins, P. Timmerman and D. N. Reinhoudt, *J. Am. Chem. Soc.*, 2001, **123**, 10153–10163.
146 M. M. Green, B. A. Garetz, B. Munoz, H. Chang, S. Hoke and R. G. Cooks, *J. Am. Chem. Soc.*, 1995, **117**, 4181–4182.
147 Y. Wada, K.-i Shinohara, H. Asakawa, S. Matsui, T. Taima and T. Ikai, *J. Am. Chem. Soc.*, 2019, **141**, 13995–14002.
148 E. Yashima, K. Maeda and Y. Okamoto, *Nature*, 1999, **399**, 449–451.
149 J. M. Rivera, T. Martín and J. Rebek, *Science*, 1998, **279**, 1021–1023.
150 J. M. Lehn and J. Sanders, *Angew. Chem.*, 1995, **34**, 2563.
151 M. A. Mateos-Timoneda, M. Crego-Calama and D. N. Reinhoudt, *Chem. Soc. Rev.*, 2004, **33**, 363–372.
152 Y. Deng, Q. Zhang, T. Nie, F. Xu, R. Costil, X.-Q. Gong, H. Tian, B. L. Feringa and D.-H. Qu, *Adv. Opt. Mater.*, 2022, **10**, 2101267.
153 D. A. Poole, S. Mathew and J. N. H. Reek, *J. Am. Chem. Soc.*, 2021, **143**, 16419–16427.
154 R. Saha, B. Mondal and P. S. Mukherjee, *Chem. Rev.*, 2022, **122**, 12244–12307.
155 C. Zhou, Y. Ren, J. Han, X. Gong, Z. Wei, J. Xie and R. Guo, *J. Am. Chem. Soc.*, 2018, **140**, 9417–9425.
156 C. Yang, L. Luo, J. Chen, B. Yang, W. Wang, H. Wang, G. Long, G. Liu, J. Zhang and W. Huang, *Chem. Commun.*, 2021, **57**, 10031–10034.
157 P. Xing, Y. Li, S. Xue, S. Z. Fiona Phua, C. Ding, H. Chen and Y. Zhao, *J. Am. Chem. Soc.*, 2019, **141**, 9946–9954.
158 Y. Meng, W. J. Xu, M. R. Newman, D. S. W. Benoit and M. Anthamatten, *Adv. Funct. Mater.*, 2019, **29**, 1903721.
159 Q. Zhang, D.-H. Qu and H. Tian, *Adv. Opt. Mater.*, 2019, **7**, 1900033.
160 J. Nie, J. Huang, J. Fan, L. Cao, C. Xu and Y. Chen, *ACS Sustainable Chem. Eng.*, 2020, **8**, 13724–13733.
161 Y. Yang and M. W. Urban, *Adv. Mater. Interfaces*, 2018, **5**, 1800384.
162 A. Jamadar and A. Das, *Polym. Chem.*, 2020, **11**, 385–392.
163 Z. Zhao, S. Zhuo, R. Fang, L. Zhang, X. Zhou, Y. Xu, J. Zhang, Z. Dong, L. Jiang and M. Liu, *Adv. Mater.*, 2018, **30**, 1804435.
164 L. Song, Z. Wang, M. E. Lamm, L. Yuan and C. Tang, *Macromolecules*, 2017, **50**, 7475–7483.
165 T. Nishimura, K. Maeda and E. Yashima, *Chirality*, 2004, **16**, S12–S22.

 This journal is © The Royal Society of Chemistry 2024

Published on 03 January 2024. Downloaded by Yunnan University on 8/4/2025 1:35:41 AM.

166 S. Burattini, B. W. Greenland, D. H. Merino, W. Weng, J. Seppala, H. M. Colquhoun, W. Hayes, M. E. Mackay, I. W. Hamley and S. J. Rowan, *J. Am. Chem. Soc.*, 2010, **132**, 12051–12058.
167 M. Carini, M. Marongiu, K. Strutyński, A. Saeki, M. Melle-Franco and A. Mateo-Alonso, *Angew. Chem., Int. Ed.*, 2019, **58**, 15788–15792.
168 T. Mes, R. van der Weegen, A. R. Palmans and E. Meijer, *Angew. Chem., Int. Ed.*, 2011, **50**, 5085–5089.
169 J. M. Paulusse and R. P. Sijbesma, *Angew. Chem., Int. Ed.*, 2004, **116**, 4560–4562.
170 W. Lu, X. Le, J. Zhang, Y. Huang and T. Chen, *Chem. Soc. Rev.*, 2017, **46**, 1284–1294.
171 Z. C. Jiang, Y. Y. Xiao, Y. Kang, M. Pan, B. J. Li and S. Zhang, *ACS Appl. Mater. Interfaces*, 2017, **9**, 20276–20293.
172 P. R. A. Chivers and D. K. Smith, *Nat. Rev. Mater.*, 2019, **4**, 463–478.
173 M. E. Lamm, Z. Wang, J. Zhou, L. Yuan, X. Zhang and C. Tang, *Polymer*, 2018, **144**, 121–127.
174 Z. Wang, Y. Zhang, L. Yuan, J. Hayat, N. M. Trenor, M. E. Lamm, L. Vlaminck, S. Billiet, F. E. Du Prez, Z. Wang and C. Tang, *ACS Macro Lett.*, 2016, **5**, 602–606.
175 V. Ayzac, Q. Sallembien, M. Raynal, B. Isare, J. Jestin and L. Bouteiller, *Angew. Chem., Int. Ed.*, 2019, **58**, 13849–13853.
176 J. Yan, M. Li, Z. Wang, C. Chen, C. Ma and G. Yang, *Chem. Eng. J.*, 2020, **389**, 123468.
177 M. Guo, L. M. Pitet, H. M. Wyss, M. Vos, P. Y. W. Dankers and E. W. Meijer, *J. Am. Chem. Soc.*, 2014, **136**, 6969–6977.
178 C. Heinzmann, U. Salz, N. Moszner, G. L. Fiore and C. Weder, *ACS Appl. Mater. Interfaces*, 2015, **7**, 13395–13404.
179 S. Tan, Y. Sha, T. Zhu, M. A. Rahman and C. Tang, *Polym. Chem.*, 2018, **9**, 5395–5401.
180 M. Liu, P. Liu, G. Lu, Z. Xu and X. Yao, *Angew. Chem., Int. Ed.*, 2018, **57**, 11242–11246.
181 K. Liu, L. Cheng, N. Zhang, H. Pan, X. Fan, G. Li, Z. Zhang, D. Zhao, J. Zhao, X. Yang, Y. Wang, R. Bai, Y. Liu, Z. Liu, S. Wang, X. Gong, Z. Bao, G. Gu, W. Yu and X. Yan, *J. Am. Chem. Soc.*, 2021, **143**, 1162–1170.
182 K. P. Nair, V. Breedveld and M. Weck, *Macromolecules*, 2011, **44**, 3346–3357.
183 A. Khan, R. R. Kisannagar, C. Gouda, D. Gupta and H.-C. Lin, *J. Mater. Chem. A*, 2020, **8**, 19954–19964.
184 X. Ji, K. Jie, S. C. Zimmerman and F. Huang, *Polym. Chem.*, 2015, **6**, 1912–1917.
185 W. Yong and H. Zhang, *Prog. Mater. Sci.*, 2021, **116**, 100713.
186 L. Michalek, S. Bialas, S. L. Walden, F. R. Bloesser, H. Frisch and C. Barner-Kowollik, *Adv. Funct. Mater.*, 2020, **30**, 2005328.
187 Q. Feng, M. Shen, J. Zhu, J. Li, J. Zhang and S. Guo, *Mater. Des.*, 2021, **212**, 110208.
188 J. Sievers, S. Zschoche, R. Dockhorn, J. Friedrichs, C. Werner and U. Freudenberg, *ACS Appl. Mater. Interfaces*, 2019, **11**, 41862–41874.
189 L. R. Rieth, R. F. Eaton and G. W. Coates, *Angew. Chem., Int. Ed.*, 2001, **40**, 2153–2156.
190 M. R. Fu, Y. You, M. Z. Rong and M. Q. Zhang, *Mater. Chem. Front.*, 2022, **6**, 52–62.
191 M. E. Lamm, L. Song, Z. Wang, M. A. Rahman, B. Lamm, L. Fu and C. Tang, *Macromolecules*, 2019, **52**, 8967–8975.
192 E. M. Foster, E. E. Lensmeyer, B. Zhang, P. Chakma, J. A. Flum, J. J. Via, J. L. Sparks and D. Konkolewicz, *ACS Macro Lett.*, 2017, **6**, 495–499.
193 J. Chen, Q. Peng, T. Thundat and H. Zeng, *Chem. Mater.*, 2019, **31**, 4553–4563.
194 H. Yuan, W. Li, C. Song and R. Huang, *Int. J. Biol. Macromol.*, 2022, **205**, 563–573.
195 C. Chen, J. Wang, S. E. Woodcock and Z. Chen, *Langmuir*, 2002, **18**, 1302–1309.
196 Y. S. Lipatov, *Prog. Polym. Sci.*, 2002, **27**, 1721–1801.
197 Y. He, S. Xiang and B. Chen, *J. Am. Chem. Soc.*, 2011, **133**, 14570–14573.
198 H. Zhang, D. Yu, S. Liu, C. Liu, Z. Liu, J. Ren and X. Qu, *Angew. Chem., Int. Ed.*, 2022, **61**, e202109068.
199 B. Wang, R. B. Lin, Z. Zhang, S. Xiang and B. Chen, *J. Am. Chem. Soc.*, 2020, **142**, 14399–14416.
200 S. B. Yu, F. Lin, J. Tian, J. Yu, D. W. Zhang and Z.-T. Li, *Chem. Soc. Rev.*, 2022, **51**, 434–449.
201 J. Wang, L. Zhao, J. Tong, Y. Yu, X. Wang and S. Yu, *Int. J. Mol. Sci.*, 2022, **23**, 4206.
202 I. Hisaki, C. Xin, K. Takahashi and T. Nakamura, *Angew. Chem., Int. Ed.*, 2019, **131**, 11278–11288.
203 S. Mehrparvar, C. Wölper, R. Gleiter and G. Haberhauer, *Angew. Chem., Int. Ed.*, 2020, **59**, 17154.
204 B. Wang, X. L. Liu, J. Lv, L. Ma, R. B. Lin, H. Cui, J. Zhang, Z. Zhang, S. Xiang and B. Chen, *Chem. Commun.*, 2020, **56**, 66–69.
205 Q. Huang, W. Li, Z. Mao, L. Qu, Y. Li, H. Zhang, T. Yu, Z. Yang, J. Zhao, Y. Zhang, M. P. Aldred and Z. Chi, *Nat. Commun.*, 2019, **10**, 3074.
206 P. Li, P. Li, M. R. Ryder, Z. Liu, C. L. Stern, O. K. Farha and J. F. Stoddart, *Angew. Chem., Int. Ed.*, 2019, **58**, 1664–1669.
207 C. A. Anderson, A. R. Jones, E. M. Briggs, E. J. Novitsky, D. W. Kuykendall, N. R. Sottos and S. C. Zimmerman, *J. Am. Chem. Soc.*, 2013, **135**, 7288–7295.
208 Y. Zhang and S. C. Zimmerman, *Beilstein J. Org. Chem.*, 2012, **8**, 486–495.
209 A. Ahagon and A. Gent, *J. Polym. Sci., Part B: Polym. Phys.*, 1975, **13**, 1285–1300.
210 Y. Zhang, C. A. Anderson and S. C. Zimmerman, *Org. Lett.*, 2013, **15**, 3506–3509.
211 X. Liu, Q. Zhang, Z. Gao, R. Hou and G. Gao, *ACS Appl. Mater. Interfaces*, 2017, **9**, 17645–17652.
212 X. Wang, Y. Li, Y. Qian, H. Qi, J. Li and J. Sun, *Adv. Mater.*, 2018, **30**, e1803854.
213 X. Li, J. Lai, Y. Deng, J. Song, G. Zhao and S. Dong, *J. Am. Chem. Soc.*, 2020, **142**, 21522–21529.
214 W. Hong, J. Lin, X. Tian and L. Wang, *Polymer*, 2021, **235**, 124301.
215 L. Wang, Z. Yin, Y. Zhang, Y. Jiang, L. Zhang and A. Yasin, *RSC Adv.*, 2018, **8**, 21798–21805.
216 Y. Tian, J. Wu, X. Fang, L. Guan, N. Yao, G. Yang, Z. Wang, Z. Hua and G. Liu, *Adv. Funct. Mater.*, 2022, **32**, 2112741.

Published on 03 January 2024. Downloaded by Yunnan University on 8/4/2025 1:35:41 AM.

217 J. Courtois, I. Baroudi, N. Nouvel, E. Degrandi, S. Pensec, G. Ducouret, C. Chaneac, L. Bouteiller and C. Creton, *Adv. Funct. Mater.*, 2010, **20**, 1803–1811.
218 S. Zou, H. Schönherr and G. J. Vancso, *J. Am. Chem. Soc.*, 2005, **127**, 11230–11231.
219 N. Hosono, A. M. Kushner, J. Chung, A. R. Palmans, Z. Guan and E. Meijer, *J. Am. Chem. Soc.*, 2015, **137**, 6880–6888.
220 S. Zou, H. Schönherr and G. J. Vancso, *Angew. Chem., Int. Ed.*, 2005, **44**, 956–959.
221 M. Pierce, J. Stuart, A. Pungor, P. Dryden and V. Hlady, *Langmuir*, 1994, **10**, 3217–3221.
222 H. Clausen-Schaumann, M. Rief, C. Tolksdorf and H. E. Gaub, *Biophys. J.*, 2000, **78**, 1997–2007.
223 G. U. Lee, L. A. Chrisey and R. J. Colton, *Science*, 1994, **266**, 771.
224 G. U. Lee, D. A. Kidwell and R. J. Colton, *Langmuir*, 1994, **10**, 354–357.
225 V. T. Moy, E. L. Florin and H. E. Gaub, *Science*, 1994, **266**, 257–259.
226 M. Rief, H. Clausen-Schaumann and H. E. Gaub, *Nat. Struct. Mol. Biol.*, 1999, **6**, 346–349.
227 P. Hinterdorfer, F. Kienberger, A. Raab, H. J. Gruber, W. Baumgartner, G. Kada, C. Riener, S. Wielert-Badt, C. Borken and H. Schindler, *Single Mol.*, 2000, **1**, 99–103.
228 R. Merkel, P. Nassoy, A. Leung, K. Ritchie and E. Evans, *Nature*, 1999, **397**, 50–53.
229 E. Evans, *Annu. Rev. Biophys. Biomol. Struct.*, 2001, **30**, 105–128.
230 H. Schönherr, M. W. Beulen, J. Bügler, J. Huskens, F. C. van Veggel, D. N. Reinhoudt and G. J. Vancso, *J. Am. Chem. Soc.*, 2000, **122**, 4963–4967.
231 S. Zapotoczny, T. Auletta, M. R. de Jong, H. Schönherr, J. Huskens, F. C. van Veggel, D. N. Reinhoudt and G. J. Vancso, *Langmuir*, 2002, **18**, 6988–6994.
232 T. Auletta, M. R. de Jong, A. Mulder, F. C. van Veggel, J. Huskens, D. N. Reinhoudt, S. Zou, S. Zapotoczny, H. Schönherr and G. J. Vancso, *J. Am. Chem. Soc.*, 2004, **126**, 1577–1584.
233 E. Evans, K. Ritchie and R. Merkel, *Biophys. J.*, 1995, **68**, 2580–2587.
234 E. Evans and K. Ritchie, *Biophys. J.*, 1997, **72**, 1541–1555.
235 E. Evans and P. Williams, *Dynamic force spectroscopy in Physics of bio-molecules and cells (Physique des biomolécules et des cellules)*, ed. H. Flyvbjerg, F. Julicher, P. Ormos and F. David, Springer, Berlin, 2002, pp. 145–204.
236 R. Dong, Y. Zhou, X. Huang, X. Zhu, Y. Lu and J. Shen, *Adv. Mater.*, 2015, **27**, 498–526.
237 C. Wang, H. Sang, Y. Wang, F. Zhu, X. Hu, X. Wang, X. Wang, Y. Li and Y. Cheng, *Nano Lett.*, 2018, **18**, 7045–7051.
238 C. L. Liquori, K. Ricker, M. L. Moseley, J. F. Jacobsen, W. Kress, S. L. Naylor, J. W. Day and L. P. Ranum, *Science*, 2001, **293**, 864–867.
239 M. Mahadevan and C. Tsilfidis, *Science*, 1992, **255**, 1253.
240 J. J. Magaña and B. Cisneros, *J. Neurosci. Res.*, 2011, **89**, 275–285.
241 S. B. Krueger and S. C. Zimmerman, *J. Med. Chem.*, 2022, **65**(18), 12417–12426.
242 J. F. Arambula, S. R. Ramisetty, A. M. Baranger and S. C. Zimmerman, *Proc. Natl. Acad. Sci. U. S. A.*, 2009, **106**, 16068–16073.
243 N. Branda, G. Kurz and J.-M. Lehn, *Chem. Commun.*, 1996, 2443–2444.
244 H. Chen and L. W. McLaughlin, *J. Am. Chem. Soc.*, 2008, **130**, 13190–13191.
245 C. H. Wong, S. L. Richardson, Y. J. Ho, A. M. Lucas, T. Tuccinardi, A. M. Baranger and S. C. Zimmerman, *ChemBioChem*, 2012, **13**, 2505–2509.
246 C. H. Wong, Y. Fu, S. R. Ramisetty, A. M. Baranger and S. C. Zimmerman, *Nucleic Acids Res.*, 2011, **39**, 8881–8890.
247 A. H. Jahromi, L. Nguyen, Y. Fu, K. A. Miller, A. M. Baranger and S. C. Zimmerman, *ACS Chem. Biol.*, 2013, **8**, 1037–1043.
248 A. H. Jahromi, Y. Fu, K. A. Miller, L. Nguyen, L. M. Luu, A. M. Baranger and S. C. Zimmerman, *J. Med. Chem.*, 2013, **56**, 9471–9481.
249 A. H. Jahromi, M. Honda, S. C. Zimmerman and M. Spies, *Nucleic Acids Res.*, 2013, **41**, 6687–6697.
250 C. H. Wong, L. Nguyen, J. Peh, L. M. Luu, J. S. Sanchez, S. L. Richardson, T. Tuccinardi, H. Tsoi, W. Y. Chan and H. E. Chan, *J. Am. Chem. Soc.*, 2014, **136**, 6355–6361.
251 B. N. Trawick, A. T. Daniher and J. K. Bashkin, *Chem. Rev.*, 1998, **98**, 939–960.
252 H. Lönnberg, *Org. Biomol. Chem.*, 2011, **9**, 1687–1703.
253 J. E. Lee, C. F. Bennett and T. A. Cooper, *Proc. Natl. Acad. Sci. U. S. A.*, 2012, **109**, 4221–4226.
254 L. Guan and M. D. Disney, *Angew. Chem., Int. Ed.*, 2013, **52**, 1462–1465.
255 L. A. Coonrod, M. Nakamori, W. Wang, S. Carrell, C. L. Hilton, M. J. Bodner, R. B. Siboni, A. G. Docter, M. M. Haley and C. A. Thornton, *ACS Chem. Biol.*, 2013, **8**, 2528–2537.
256 L. Nguyen, L. M. Luu, S. Peng, J. F. Serrano, H. E. Chan and S. C. Zimmerman, *J. Am. Chem. Soc.*, 2015, **137**, 14180–14189.
257 L. M. Luu, L. Nguyen, S. Peng, J. Lee, H. Y. Lee, C. H. Wong, P. J. Hergenrother, H. Chan and S. C. Zimmerman, *ChemMedChem*, 2016, **11**, 1428–1435.
258 C. A. Lipinski, *J. Pharmacol. Toxicol. Methods*, 2000, **44**, 235–249.
259 C. T. Varner, T. Rosen, J. T. Martin and R. S. Kane, *Biomacromolecules*, 2014, **16**, 43–55.
260 R. Ribeiro-Viana, M. Sánchez-Navarro, J. Luczkowiak, J. R. Koeppe, R. Delgado, J. Rojo and B. G. Davis, *Nat. Commun.*, 2012, **3**, 1303.
261 Y. Bai, L. Nguyen, Z. Song, S. Peng, J. Lee, N. Zheng, I. Kapoor, L. D. Hagler, K. Cai and J. Cheng, *J. Am. Chem. Soc.*, 2016, **138**, 9498–9507.
262 L. D. Hagler, L. M. Luu, M. Tonelli, J. Lee, S. M. Hayes, S. E. Bonson, J. I. Vergara, S. E. Butcher and S. C. Zimmerman, *Biochemistry*, 2020, **59**, 3463–3472.
263 A. Pushechnikov, M. M. Lee, J. L. Childs-Disney, K. Sobczak, J. M. French, C. A. Thornton and M. D. Disney, *J. Am. Chem. Soc.*, 2009, **131**, 9767–9779.

 This journal is © The Royal Society of Chemistry 2024

Published on 03 January 2024. Downloaded by Yunnan University on 8/4/2025 1:35:41 AM.

264 L. D. Hagler, S. B. Krueger, L. M. Luu, A. N. Lanzendorf, N. L. Mitchell, J. I. Vergara, L. D. Curet and S. C. Zimmerman, *ACS Med. Chem. Lett.*, 2021, **12**, 935–940.
265 R. Dong, Y. Pang, Y. Su and X. Zhu, *Biomater. Sci.*, 2015, **3**, 937–954.
266 N. Song, X. Y. Lou, L. J. Ma, H. Gao and Y. W. Yang, *Theranostics*, 2019, **9**, 3075–3093.
267 M. J. Webber and R. Langer, *Chem. Soc. Rev.*, 2017, **46**, 6600–6620.
268 L. Lu, L. Yuan, J. Yan, C. Tang and Q. Wang, *Biomacromolecules*, 2016, **17**, 2321–2328.
269 Z. C. Huang, W. T. Song and X. S. Chen, *Front. Chem.*, 2020, **8**, 380.
270 D. Kalafatovic, M. Nobis, N. Javid, P. W. J. M. Frederix, K. I. Anderson, B. R. Saunders and R. V. Ulijn, *Biomater. Sci.*, 2015, **3**, 246–249.
271 H. Cheng, Y. J. Cheng, S. Bhasin, J. Y. Zhu, X. D. Xu, R. X. Zhuo and X. Z. Zhang, *Chem. Commun.*, 2015, **51**, 6936–6939.
272 D. Wang, C. Tu, Y. Su, C. Zhang, U. Greiser, X. Zhu, D. Yan and W. Wang, *Chem. Sci.*, 2015, **6**, 3775–3787.
273 D. Wang, C. Yu, L. Xu, L. Shi, G. Tong, J. Wu, H. Liu, D. Yan and X. Zhu, *J. Am. Chem. Soc.*, 2018, **140**, 8797–8806.
274 R. Cao, T. F. Liu, Q. Yin, Z. Peng and J. Lü, *Angew. Chem., Int. Ed.*, 2018, **57**, 7691–7696.
275 Y. H. Luo, X. T. He, D. L. Hong, C. Chen, F. H. Chen, J. Jiao, L. H. Zhai, L. H. Guo and B. W. Sun, *Adv. Funct. Mater.*, 2018, **28**, 1804822.
276 X. T. He, Y. H. Luo, D. L. Hong, F. H. Chen, Z. Y. Zheng, C. Wang, J. Y. Wang, C. Chen and B. W. Sun, *ACS Appl. Nano Mater.*, 2019, **2**, 2437–2445.
277 N. Mehwish, X. Dou, Y. Zhao and C. L. Feng, *Mater. Horiz.*, 2019, **6**, 14–44.
278 Y. V. Gerasimova, S. Peck and D. M. Kolpashchikov, *Chem. Commun.*, 2010, **46**, 8761–8763.
279 S. Zhu, Z. Liu, W. Zhang, S. Han, L. Hu and G. Xu, *Chem. Commun.*, 2011, **47**, 6099–6101.
280 J. Luo, Z. Xie, J. W. Lam, L. Cheng, H. Chen, C. Qiu, H. S. Kwok, X. Zhan, Y. Liu and D. Zhu, *Chem. Commun.*, 2001, 1740–1741.
281 J. Mei, N. L. Leung, R. T. Kwok, J. W. Lam and B. Z. Tang, *Chem. Rev.*, 2015, **115**, 11718–11940.
282 B. Li, T. He, X. Shen, D. Tang and S. Yin, *Polym. Chem.*, 2019, **10**, 796–818.
283 X. Lou, C. W. T. Leung, C. Dong, Y. Hong, S. Chen, E. Zhao, J. W. Y. Lam and B. Z. Tang, *RSC Adv.*, 2014, **4**, 33307–33311.
284 S. Wang, D. Wei, Z. Zhu and C. Yang, *Sens. Actuators, B*, 2016, **235**, 280–286.
285 L. Teng, Y. Chen, Y.-G. Jia and L. Ren, *J. Mater. Chem. B*, 2019, **7**, 6705–6736.
286 Y. Zhao, S. Song, X. Ren, J. Zhang, Q. Lin and Y. Zhao, *Chem. Rev.*, 2022, **122**(6), 5604–5640.
287 M. Matsusaki, R. Amekawa, M. Matsumoto, Y. Tanaka, A. Kubota, K. Nishida and M. Akashi, *Adv. Mater.*, 2011, **23**, 2957–2961.
288 L. Han, M. Wang, P. Li, D. Gan, L. Yan, J. Xu, K. Wang, L. Fang, C. W. Chan, H. Zhang, H. Yuan and X. Lu, *ACS Appl. Mater. Interfaces*, 2018, **10**, 28015–28026.
289 S. Liu, D. Qi, Y. Chen, L. Teng, Y. Jia and L. Ren, *Biomater. Sci.*, 2019, **7**, 1286–1298.
290 P. Y. W. Dankers, M. C. Harmsen, L. A. Brouwer, M. J. A. Van Luyn and E. W. Meijer, *Nat. Mater.*, 2005, **4**, 568–574.
291 P. Y. W. Dankers, E. N. M. van Leeuwen, G. M. L. van Gemert, A. J. H. Spiering, M. C. Harmsen, L. A. Brouwer, H. M. Janssen, A. W. Bosman, M. J. A. van Luyn and E. W. Meijer, *Biomaterials*, 2006, **27**, 5490–5501.
292 X. Zhao, Y. Liang, Y. Huang, J. He, Y. Han and B. Guo, *Adv. Funct. Mater.*, 2020, **30**, 1910748.
293 X. Hu, N. Wang, L. Liu and W. Liu, *J. Biomater. Sci., Polym. Ed.*, 2013, **24**, 1869–1882.
294 D. E. Liu, J. An, C. Pang, X. Yan, W. Li, J. Ma and H. Gao, *Macromol. Biosci.*, 2019, **19**, 1800359.
295 N. Shao, T. Dai, Y. Liu and Y. Cheng, *Chem. Commun.*, 2015, **51**, 9741–9743.
296 W. Shen, Q. Wang, Y. Shen, X. Gao, L. Li, Y. Yan, H. Wang and Y. Cheng, *ACS Cent. Sci.*, 2018, **4**, 1326–1333.